To the Graduate Council:

I am submitting herewith a dissertation written by Carla S. Sommardahl entitled "Molecular and Genetic Analysis of the *orpk* Mouse Model of Polycystic Kidney Disease: Searching for Treatments and Modifier Genes." I have examined the final copy of this dissertation for form and content and recommend that it be accepted in partial fulfillment of the requirements for the degree of doctor of Philosophy, with a major in Comparative Experimental Medicine.

J. Erby Wilkinson, Major Professor

We have read this dissertation
and recommend its acceptance:

Dabney K. Johnson

David O. Slauson

Edward J. Michaud

Accepted for the Council:

Associate Vice Chancellor and
Dean of the Graduate School

Molecular and Genetic Analysis of the *orpk* Mouse Model of Polycystic Kidney Disease: Searching for Treatments and Modifier Genes

A Dissertation

Presented for the

Doctor of Philosophy

Degree

The University of Tennessee, Knoxville

Carla S. Sommardahl

December 1999

DEDICATION

This dissertation is dedicated to my parents who gave me the genes and environment to succeed in all my educational endeavors. Also, to my husband, whose encouragement and help during these past very busy years, has enabled me to reach this goal.

ACKNOWLEDGEMENTS

I would like to thank Dr. Erby Wilkinson, my major professor for all his help and encouragement toward this degree. I would also like to thank the other members of my Dissertation Committee, Dabney Johnson, who has guided me in my research and who I hope continues to guide me; Dave Slauson, who is always encouraging and understands my clinical perspective; and Ed Michaud, who agreed to be a committee member at the last minute, but who has been a friend and mentor for several years.

There are many people who assisted me in my work and I would like to recognize and show my appreciation. I would like to thank Marilyn Cottrell and Nancy Neilsen for all their technical help and advice. I thank the Department of Pathology and the Department of Large Animal Clinical Sciences for allowing me to be a graduate student and clinician at the same time. This allowed me to maintain my skills as a veterinarian while I learned new skills as a researcher. I have received generous financial support from the College of Veterinary Medicine Center of Excellence and by the National Institute of Health National Institute of Diabetes and Digestive and Kidney Disease grant #K08DK02466. Lastly, I would like to thank Deb Haines and Tommy Jordan for all their help in the preparation of the figures and photographs in this dissertation.

Abstract

The *orpk* line of mice was previously identified as a unique model for human polycystic kidney disease. The most prominent phenotype is the invariable development of bilateral polycystic kidneys and abnormalities in the intrahepatic biliary tract and pancreas.

Taxol has been reported to be of therapeutic benefit in the *cpk* mouse model of polycystic kidney disease. The effects of taxol treatment on the development of renal cysts and biliary dysplasia/hyperplasia in the *orpk* mouse mutant were studied. There were no significant differences between the treatment and control groups with respect to weight gain, survival, urine to serum osmolality ratio, and serum concentration of liver enzymes. Moreover, the renal cystic development and biliary hyperplasia was not affected by taxol treatment in the *orpk* mutant animals.

There are marked differences in the phenotypic expression of the *orpk* mutation when bred on different genetic backgrounds. In the FVB/N genetic background, the phenotype is very severe in the kidney, liver, and pancreas lesions. To better evaluate how genetic background might influence the expressivity of the *orpk* phenotype, the transgene was made congenic on the C3H genetic background. Congenic *orpk*-C3H mutant mice have a much less sever phenotype identical to that initially observed in the first generation backcross to C3H. The kidney lesions are morphologically similar in the *orpk*-C3H mutant mice, but they develop renal cysts at a slower rate and have fewer cysts at all stages of cyst development. These animals also retain their renal

concentrating ability. The liver lesions in the *orpk*-C3H mutant animals are less aggressive and are characterized by multifocal biliary hyperplasia, dysplasia, and portal fibrosis isolated to the portal triad regions. The significant lesions when the *orpk* mutation is on a different genetic background suggests the presence of important modifier genes that vary in the FVB/N and C3H genetic backgrounds.

Whole genome quantitative trait analysis was performed to determine the chromosomal location of the modifier genes that influence the phenotypic expression of the *orpk* in the FVB/N and C3H genetic backgrounds. The percent of the kidney that is cystic was used as a quantitative trait that reflects the kidney phenotype. Serum concentration of alkaline phosphatase was used as a quantitative trait that reflects the liver phenotype. A backcross between (*orpk*-FVB X C3H) F1 tg/+ mice and *orpk*-FVB tg/+ mice was performed and 100 tg/tg progeny were scored for the kidney and liver traits.

Whole genome quantitative trait loci mapping of 40 selected backcross tg/tg progeny (20 with mild kidney scores and 20 with severe kidney scores) identified three chromosomal intervals that segregated with the severe kidney phenotype. Whole genome quantitative trait loci mapping of 40 selected backcross tg/tg progeny (20 with mild liver scores and 20 with severe liver scores) identified one DNA marker that segregated with the severe liver phenotype. Further characterization of these intervals with low resolution and fine mapping may provide candidate modifying loci that will provide information in understanding the pathogenesis of polycystic kidney disease.

TABLE OF CONTENTS

LIST OF FIGURES

LIST OF ABBREVIATIONS

ADPKD	autosomal dominant polycystic kidney disease
ALP	alkaline phosphatase
ARPKD	autosomal recessive polycystic kidney disease
ALT	alanine transaminase
BC	backcross
bpk	BALB/c polycystic kidneys
BWt	body weight
CFTR	cystic fibrosis transmembrane receptor
cM	CentiMorgan (1% recombination or one map unit)
cpk	congenital polycystic kidneys
DMSO	dimethyl sulfoxide
ECM	extracellular matrix
EGFR	epidermal growth factor receptor
jck	juvenile cystic kidneys
jcpk	juvenile congenital polycystic kidney
kb	kilobase(s)
NIH	National Institute of Health
orpk	Oak Ridge polycystic kidney
PCR	polymerase chain reaction
pcy	polycystic kidneys
PKD	polycystic kidney
QTL	quantitative trait loci
SSLP	simple sequence length polymorphism
TPR	tetratricopeptide repeat
Usom:Sosm	urine osmolality to serum osmolality ratio
WT	wildtype

I. INTRODUCTION

Polycystic Kidney Disease

Description and incidence

The formation of renal cysts is common to several genetic disorders in humans [1-3]. As a group, polycystic kidney diseases (PKD) account for over 10% of all patients requiring chronic dialysis or kidney transplantation [2;4]. The predominant form of renal cystic disease in humans is autosomal dominant polycystic kidney disease (ADPKD), which affects approximately 1 in 1,000 individuals and does not become evident until age 50 or more in most individuals [5;6]. This disease often has extrarenal manifestations in the liver, cardiovascular system, and gastrointestinal tract [7]. Autosomal recessive polycystic disease (ARPKD) is a more aggressive disorder, which presents late in fetal development or shortly after birth. The estimated incidence of this disease in the human population is 1 in 6,000 to 1 in 55,000 live births with a carrier frequency of approximately 1:49 [2]. ARPKD is characterized by renal collecting tubule ectasia, hepatic portal fibrosis, and biliary dysgenesis [8;9]. Clinical complications of the kidney and liver pathology in patients with ARPKD who survive the neonatal period include systemic hypertension, renal failure, portal hypertension and ascending cholangitis. A locus for ARPKD has been localized to chromosome 6 and appears to be the primary locus associated with ARPKD in humans [10;11]. The gene associated with ARPKD, however, has yet to be identified.

Mouse models for Polycystic Kidney Disease

Animal models of the various forms of human cystic disease have contributed greatly to our understanding of the pathogenesis of these kidney disorders [12-16]. The recessive *cpk* (congenital polycystic kidneys) mutation in mice has been examined in considerable detail [17;18]. Additional spontaneous recessive mutations in mice – *bpk* (BALB/c polycystic kidneys), *pcy* (polycystic kidneys), *jck* (juvenile cystic kidneys), *nml633*, and *jcpk* (juvenile congenital polycystic kidney) - have been reported [16;19-22]. The cystic disease that develops in the *pcy* and *nml633* models resembles human ADPKD and the cystic disease that develops in the *cpk, bpk, jcpk,* and *jck* models shows similarities to clinical features of human ARPKD [23-25]. The dual hepatorenal pathology that is a hallmark feature of human ARPKD has been reported as a feature only in the *bpk* mouse [25]. However, in this model, the hepatic pathology is mild or absent dependent on the genetic background of the animal. Attempts to identify the genes associated with these mutations have been restricted by the fact that there are no DNA probes available that are directly associated with the mutant locus in any of these animals.

Our model of PKD is a recessive mouse mutation that causes a form of polycystic kidney disease that closely resembles human ARPKD [26]. This mutation arose by insertional mutagenesis in one line of transgenic mice and is named *orpk* (Oak Ridge polycystic kidney). In contrast to the other animal models for renal cystic disease, the mutant locus could be cloned using the exogenously added transgene as a "molecular tag". The *orpk* mutation arose as part of a large-scale insertional mutagenesis program at the Oak Ridge National Laboratory. This line was generated on the FVB/N inbred genetic background by

pronuclear microinjection of a transgene construct containing the bacterial chloramphenicol acetyltransferase gene under the control of a mutated version of the polyoma early region promoter. The abnormal phenotype is the result of disruption of an endogenous gene (*Tg737*) and is not associated with the nonexpressed transgene product. Therefore, the phenotype in the *orpk* line occurs only among transgenic homozygotes derived from crosses between animals hemizygous for the transgene [26]. The mutation is passed from one generation to another in a simple Mendelian manner and the phenotype in homozygotes appears to be 100% penetrant since all animals identified by genotypic analysis as transgenic homozygotes are similarly affected. No mutant traits are detected in animals heterozygous for the transgene [26].

Phenotype of the *orpk* mutant animals

The *orpk* mutant phenotype on the FVB/N genetic background is very severe with a majority of the affected animals dying within a few weeks after birth [26;27]. FVB/N *orpk* mutants have scruffy fur, are severely growth retarded and also exhibit skeletal abnormalities. The most prominent aspect of the phenotype involves the invariable development of bilateral polycystic kidney disease and abnormalities associated with the intrahepatic biliary tract [26;28;29]. Gross examinations of mutant kidneys revealed that they were slightly enlarged, pale, and contained numerous cysts with concurrent destruction of the surrounding parenchyma. The livers are slightly pale with a prominent reticular pattern.

Histologically, the lesions in the kidneys and livers of *orpk* mutant mice are remarkably similar to those seen in human ARPKD. The cardinal features of both the kidney lesion (collecting tubule ectasia) and the liver lesion (biliary dysplasia

and/or portal hepatic fibrosis) typical of human ARPKD are a constant finding of the disease in the mutant animals. In the kidneys, initial mild, multifocal microscopic dilation of the proximal tubules is followed rapidly by marked dilation and cyst formation to the collecting tubules. Lectin profiling was performed on a total of 12 *orpk* mutants ranging in age from day 1 to day 28. In newborn animals, microcystic lesions were localized to proximal tubules. By postnatal day seven, cystic lesions were detected in collecting tubules, and a progressive shift in cyst localization from the proximal tubules to the collecting ducts was characteristic of all subsequent developmental stages [26]. This shift from proximal tubules to collecting duct cysts is similar to that which is observed in the *bpk* and *cpk* mutants [18]. In addition, the advanced lesions in human patients with ARPKD are located within the collecting tubules and ducts, while proximal tubule cysts are the prominent features detected at early stages of the disease [18]. The *orpk* mutants also have urine with low specific gravity (hyposthenuric) indicating that the renal concentrating ability is compromised. Serum creatinine and urea nitrogen concentration, however, are normal in these animals.

As with the renal lesion, the hepatic abnormality detected in the *orpk* mutants is similar to that observed in humans with ARPKD. A prominent feature in both is an abnormality in the intrahepatic biliary tract involving primarily the bile ducts and ductules. The liver lesion on the FVB/N genetic background is characterized by the proliferation of poorly differentiated epithelial cells emanating from the portal triads and the formation of primitive, dysplastic, tortuous ductules that expand the portal periportal areas. These cells can ultimately disrupt the limiting plate, isolate individual hepatocytes, and can give rise to anastomosing tortuous bile ductules in the end-stage diseased liver [26;28]. Serum concentrations of

liver enzymes, specifically alkaline phosphatase (ALP) and alanine transaminase (ALT), and bile acids are elevated compared to normal FVB/N mice. The most marked elevation is in ALP and bile acids supporting the biliary tract origin of the liver lesion. The mutant animals in the FVB/N genetic background also develop a pancreatic lesion characterized by pancreatic ductule hyperplasia and proliferation with fibrosis and acinar cell atrophy. The islet of Langerhans cells appear unaffected by the lesions, but are less numerous.

To evaluate how genetic background might influence the expressivity of the *orpk* phenotype, the mutant locus was made congenic on the C3HeB/FeJLe inbred genetic background (*orpk*-C3H line). As in human ARPKD, the pathologic features of the *orpk* phenotype include a spectrum of disease with variable severity in which the primary lesions of the kidneys and liver are expressed to different degrees. Congenic *orpk*-C3H mutant mice have a much less severe phenotype. This dramatic decrease in severity is evident in first generation backcross to C3H. Initial experiments clearly show that these animals live much longer (weeks to months vs. days to weeks), develop renal cysts at a slower rate, and have a less aggressive liver disease [26]. The significant difference in the lesions on a different genetic background indicates the presence of important modifier genes that vary in the FVB/N and C3H genetic backgrounds. This may also be the case in human ARPKD, in which the severity of the phenotype and the nature of the liver lesion can be quite variable.

Molecular biology of PKD

Only three genes associated with mutations that cause PKD have been cloned. Two of these are linked to the most common forms of ADPKD in humans

(*PKD1* and *PKD2*) [30;31]. The third gene is associated with the *orpk* mouse model for ARPKD [26]. The gene associated with the predominant form of ARPKD has yet to be cloned; however, the ARPKD locus has been mapped to a 1-cM interval of chromosome 6 in humans [32]. Characterization of the *orpk* mutant locus led to the identification of the *Tg737* gene that encodes an 824-amino acid polypeptide. The interrupted gene at the mutant locus in the *orpk* line contains a motif common to several genes involved in cell cycle control. This motif encodes an internally repeated 32-amino acid sequence referred to as the tetratricopeptide repeat (TPR). The TPR was first described in lower eukaryotes as a motif associated with several genes involved in cell cycle control, and recently, has been identified in proteins that mediate protein-protein interactions and function in key regulatory pathways [33-35]. The Tg737 protein has recently been shown to interact with polycystin 1, the protein product of the *PKD1* gene [36]. This finding provides molecular evidence for a common disease pathway between an animal model for ARPKD and the dominant disease in humans. It has been theorized that the proteins may exist in a common macromolecular complex in renal epithelia regulating growth, differentiation, and polarization [37;38]. The Tg737 protein has also been shown to interact with other proteins involved in epithelial cell polarity, TGF-α/EGF receptor (EGFR) stability and cellular differentiation [36].

Mechanisms of cystogenesis

Cyst formation in the kidney appears to be the final common pathway for a large number of genetic and acquired diseases. In the recent years, numerous general mechanisms and a few specific alterations have been identified that

result in cyst generation. Several studies have focused on the cellular mechanisms of cyst formation in humans and in animal models of polycystic kidney diseases. An important finding from these studies is that many features of the cyst are common to a variety of disorders. Three factors have been associated with cystogenesis in these studies; epithelial hyperplasia, secretion, and extracellular matrix (ECM) abnormalities. ECM abnormalities include changes in the expression of several components, such as matrix metalloproteinases and cysteine proteinases that regulate active remodeling and degradation of the ECM [19;39-41]. Tubular secretion is required to maintain the cyst after development. Chloride secretion through the cystic fibrosis transmembrane receptor (CFTR), persistence of a transient developmental phenotype in cystic epithelia, and physical properties of mechanical deformation are all proposed mechanisms that lead to net secretion in cystogenesis [42-44]. In all cases, the cystic structures arise from a localized proliferation of cells in different sections of the nephron depending on the specific form of the disease [45-47]. Numerous molecular defects have been associated with the hyperplasia in tubular epithelial cells including proto-oncogene activation or overexpression, growth factor and growth factor receptor dysregulation, and abnormalities in apoptosis [48-51]. Evidence from several studies has shown a direct role of the EGFR axis in the pathophysiology of PKD [37]. The EGFR has been shown to be over expressed and mislocalized in the cystic epithelium of human ARPKD and in several models of PKD, including the *orpk* mouse mutant [52-54]. These ongoing studies provide clues to the determination of the pathways and components responsible for the pathogenesis of cyst formation and may lead to possible therapeutic applications.

Therapeutic applications

There is no specific therapy to ameliorate the progression of PKD in humans. The understanding of the cellular and molecular events that trigger the formation of renal cysts and extrarenal lesions in human patients and animal models of PKD will aid in the development of potential treatments. Taxol, an antimicrotubule drug that interferes with the depolymerization of microtubules and thereby blocks cell division, has been shown to be useful against several types of malignant neoplasm [39]. Taxol has been shown to be of therapeutic benefit in the *cpk* mouse model of PKD, but not in other rodent models of PKD [55;56]. This difference in therapeutic benefit may be due to the differences in the mutations at the cellular and molecular level, or due to genetic background differences that influence the effectiveness of taxol. These factors must be taken into consideration with any potential therapeutic agent and tested in several animal models before conclusions can be made towards its benefits in humans.

I have investigated the efficacy of taxol in the *orpk* mouse model of PKD [57]. This investigation is presented in Chapter II of this manuscript. Dietary factors, such as protein and fatty acids, have also been studied to determine their effects on the progression of polycystic kidney disease in animal models [58;59]. Recently, a novel tyrosine kinase inhibitor, EKI-785, has been shown to inhibit collecting tubule cystic lesions in an organ culture system [60]. The understanding of the pathophysiology of PKD aids not only in finding potential therapeutics, but also in the search for modifier genes that have been shown to vary the phenotypic expression in human PKD and animal models of PKD. The mapping and cloning of modifier genes that influence the disease process in PKD, in turn, will aid in finding potential therapeutics.

Polygenic Inheritance

Definitions

Characteristics whose phenotypic variation is continuous and determined by the segregation of multiple loci have often been referred to as polygenic traits and the inheritance as polygenic. Polygenic traits may be classified as discrete traits that are measured by a specific outcome such as the development of a certain disease or characteristic [61]. Discrete traits may represent a threshold effect that is produced whenever an underlying quantitative variable, influenced by multiple genes, exceeds a critical threshold. Discrete traits may also be a pure synthetic effect that requires a simultaneous and joint action of several mutations. Polygenic traits may also be classified as quantitative traits that are measured by a continuous variable and are assessed quantitatively such as plant height, milk production, or blood pressure. The individual loci controlling a quantitative trait are referred to as polygenes or quantitative trait loci (QTL) [62]. The combined action of individual QTL sets the level of these traits. This form of polygenic inheritance determines most of the phenotypic characteristics that distinguish different individuals within a natural population. Quantitative traits can be described numerically based on the result of an appropriate form of measurement. Non-genetic factors can also play a role in the continuous variation in expression of a trait. Non-genetic factors are environmental or a matter of chance. Genetic and non-genetic contributions can be separated through the analysis and comparison of animals within and between inbred strains. The analysis of quantitative traits is a subspecialty of genetics called quantitative genetics, and deals with polygenes or modifier genes that determine

the variation in the phenotype. Polygenic inheritance can also refer to multiple genes that are involved in the variation of a specific disease phenotype. Phenotypic variation is demonstrated in many animal models when "genetic background" effects represent the action of modifier genes. Modifier genes explain, in part, the variability in the phenotypic expression of the same mutation within a single gene between two different strain backgrounds. The modifying genes do not have a mutation themselves, but are normal allelic variants that affect how the mutated gene is expressed or how it causes the disease. Phenotypic variability can be demonstrated as susceptibility or resistance to a disease phenotype, or as a dramatic difference in the disease pathophysiology[61]. Modifier genes are distinct from the disease-causing genes and may be located on entirely different chromosomes. Mapping of these modifier genes can provide tools for understanding the pathophysiology of the disease itself, and new tools for diagnostic and therapeutic interventions.

Mapping of QTL

Researchers over the past several years have been successful in detecting and mapping loci affecting polygenic traits in humans, animal models, and agricultural species [63]. Genome-wide QTL analysis was first performed in plants, but was soon used in mammals. The initial requirements for QTL analysis are the availability of inbred strains, a quantitative trait that can be measured numerically, a difference in expression of the quantitative trait between the inbred strains chosen, and a method to map the QTL to a chromosomal location using molecular markers. A QTL analysis can be described in three stages: detection, map estimation, and fine mapping [63]. Stage 1, the detection

stage, can locate the major QTL on chromosomes, determine the number of QTL segregating, and estimate the additive and dominance effects. Stage 2, the map estimation stage, localizes the QTL to intervals on the chromosomes. Stages 1 and 2 are performed using a genome wide scan and various statistical methods. Stage 3, the fine mapping stage, focuses on a single-QTL oriented mapping within an interval previously identified to contain a modifier locus. Stage 3 has been difficult to achieve and the experimental designs have not been well tested. This difficulty has been the reason for the lack of success in positional cloning and positional candidate gene identification in QTL analysis.

The mapping of modifier genes that control a disease phenotype among mouse inbred genetic lines can now be performed with greater ease due to advances in genetic mapping. With the advent of simple sequence repeat DNA markers (SSLP) that are distributed throughout the entire mouse genome, the QTL that contribute to a specific phenotype can now be mapped [64;65]. Currently, there are more that 6000 PCR-based highly polymorphic markers available for the mouse [65]. The markers are spaced along the genomic map to an average of less than 0.25cM (≅500 kb). Between any two inbred strains, an average of 50% of the markers are polymorphic, making it possible to map to a resolution of less than 1 cM for any trait. These markers are utilized in the genome scan for stages 1 and 2 of the QTL analysis. In stage 1, the frequency with which a set of genetic markers specific to one of the parental strains is inherited with the phenotype of interest is measured, and linkage can be established to the loci involved in modifying that phenotype. This is taken a step further in stage 2 of the QTL analysis with interval mapping. Interval mapping uses phenotypic and genetic marker information to estimate the probable

genotype and the most likely QTL effect at every point in the genome, by means of a maximum-likelihood linkage analysis. This analysis is initially done on the same population as in stage 1, but uses different statistical methods. Specific software, such as Mapmaker/QTL, has been designed to estimate QTL map location [66].

In animal models with inbred strains, the most common experimental designs used to perform the initial genome scan are the intercross (F2) and the backcross (BC). The BC matings have proven more efficient in detecting the major QTL because each BC offspring will have one of only two genotypes at each locus. There is also less genetic variance in the BC design [63]. However, if the goal is to know the number of QTL and estimate their additive and dominance effects, then the F2 design is superior. The most important consideration in choosing the inbred parental strains for either design is that they should show the greatest difference possible in the expression of the quantitative trait. After choosing the inbred parental strains, a cross to obtain F1 hybrid offspring should be performed and the quantitative trait analyzed in this population. This analysis will aid in determining whether the putative QTL are dominant, semidominant, or more complex in one strain versus the other. The mean expression of the F1 population will also aid in determining which parental strain to perform the backcross [67]. Mating F1 animals generates the F2 progeny. Once the backcross and/or F2 progeny are obtained, they are then analyzed for expression of the quantitative trait with the same method used for the F1 and parental strains. These progeny are typed for DNA or molecular markers that span the genome, such as simple sequence repeat DNA markers. These molecular markers should be spaced at intervals of 15-25 cM for the

detection and interval mapping stages of the analysis [62]. In order to save time and expense of assaying molecular markers for such a large population of animals, a modified approach has been developed to detect QTL. In this approach, marker analysis is only performed on the progeny from the extreme tails of the distribution. This is referred to as selective genotyping and only the progeny with the highest and lowest values for the quantitative trait are genotyped for the molecular markers in the genome scan. If the allele frequency at any molecular marker locus differs significantly between the two extreme subpopulations, then a QTL controlling the quantitative trait of interest may be located near the marker [62]. The drawbacks of this method are that more animals must be analyzed for the quantitative phenotype in order to have enough animals in the distribution extremes. It is also more difficult to determine individual QTL effects and to map more that one quantitative trait using this method [62]. However, if the goal is to detect the major QTL for one quantitative trait, then the benefits outweigh the penalties when using this method.

Hypothesis and Specific Aims

The hypothesis and specific aims of this project involved different aspects and methods in understanding the pathophysiology of polycystic kidney disease in the *orpk* mouse model.

1. Hypothesis: Agents that block cell division, such as taxol, will decrease the renal cystogenesis and biliary epithelial proliferation in the *orpk* mutant animals.

Specific Aim: To determine the effect of paclitaxel on cystic kidney and liver lesions in the *orpk* mutant line.

2. Hypothesis: Genetic modifiers influence the expression of the *orpk* phenotype between different mouse strains.

Specific Aim: To identify the phenotypic variations of the *orpk* mutation on the C3H genetic background.

3. Hypothesis: There are several modifier genes varying the severity of the kidney and liver lesions in the *orpk* mutants between the FVB/N and C3H genetic backgrounds.

Specific Aim: To determine the chromosomal location of the modifier genes that vary the phenotypic expression of *orpk* between the FVB/N and C3H genetic backgrounds.

II. EFFICACY OF TAXOL IN THE *ORPK* MOUSE MODEL OF POLYCYSTIC KIDNEY DISEASE

Introduction

There is no specific therapy to ameliorate the progression of ARPKD in humans. Taxol, an antimicrotubule drug that interferes with the depolymerization of microtubules and thereby blocks cell division, has been shown to be useful against several types of malignant neoplasm [39]. A previous study showed that taxol slowed the progression of renal cyst formation in the *cpk* mouse model of PKD [55]. Most notably, the treated *cpk* animals had an increased survival rate over nontreated animals. To determine whether this is a generalized effect of taxol that is applicable to other forms of PKD, we tested whether mouse mutants other than *cpk* animals also respond to this drug. Here we demonstrate that treatment with taxol has no effect on the development of renal cysts in the *orpk* mutant line. Moreover, careful analysis of the livers in the *orpk* mutants revealed that taxol also has no obvious beneficial effect on the liver lesions that develop in these animals.

Materials and Methods

Animals

Three treatment groups were established, each consisting of 10 *orpk* mutant mice and 10 wild-type control mice. Group 1 received taxol in dimethyl sulfoxide

(DMSO) at 10 μg/g body weight (BWt) weekly via an intraperitoneal injection. Group 2 received only DMSO and Group 3 received only PBS, both at equal volume/g BWt. and dosing interval as Group 1. All treatments began at 7 days of age. The mice were maintained with their parents until they were weaned at 24 days of age and genotyped for the transgene using a PCR based protocol. All mice were weighed twice weekly and sacrificed when near death or by 50 days of age.

Serum and urine analysis

Serum concentrations of alkaline phosphatase (ALP), and alanine transaminase (ALT) were measured to assess liver damage in three mutant mice of Group 1, three mutant mice of Group 2, two mutant mice of Group 3 and all control mice. Urine osmolality was measured and the urine osmolality to serum osmolality (Uosm:Sosm) ratio was calculated to assess renal concentrating ability in three mutant mice of Group 1, three mutant mice of Group 2, two mutant mice of Group 3, and all control mice. A complete blood count was performed on all control animals. Serum samples were analyzed by an Abbott spectrum chemistry analyzer, and serum and urine osmolality were measured by a Wescor vapor pressure osmometer.

Light microscopy

For histological analysis, kidneys and livers were obtained from mutant and control animals at necropsy. The tissue was fixed in 10% buffered formalin for 24-48 hours and embedded in paraffin. Sections of 5μm were mounted on glass slides and stained with hematoxylin and eosin.

Determination of cystic index

Cyst localization was studied by segment-specific lectin binding using *Dolichos biflorus* as a marker specific for collecting tubules and *Lotus tetragonolobus* as a marker specific for proximal tubules. Processing and immunostaining of tissues was performed as previously described using a post-embedding technique specifically developed for immunolocalization of antigens and lectins in plastic sections [68]. Following routine histological preparation, 6-10 regularly spaced, 3μm sections of kidneys were graded for cyst formation using an eyepiece micrometer on a scale of 0 (no observable cysts) through 4 (multiple cysts larger than 0.2 mm). The cystic index was then calculated as the mean of individual cyst scores.

Immunohistological localization of the Epidermal Growth Factor Receptor (EGFR)

The cellular localization of the EGFR was determined by immunohistological staining of mutant kidney sections with monoclonal EGFR antibodies, F-4 (Sigma. St. Louis, MO, USA) or HB 8506 (American Type Culture Collection, Rockville, MD, USA) or Rabbit antiserum, RK-2 as described [53;68;69].

Statistical analysis

Utilization of 10 animals in each treatment group was based on the following power analysis: assuming treatment would double length of survival, at an alpha level of 0.01, the power of this study is 0.94, and at an alpha level of 0.05, the power of this study is 0.97 (Solo Power Analysis, BMDP Statistical Software, Inc, Los Angeles, CA). An estimate of the mean (SEM) biweekly body weight, age at

death, ALP and ALT values, and serum osmolality to urine osmolality ratio values for control and mutant animals of each treatment group were made. A paired *t*-test was used to determine differences between treatment groups for these values. A paired *t*-test was used to determine differences between treatment groups for cystic index. Statistical significance was considered at $p<0.05$.

Results

We tested whether the effects of taxol on renal cystogenesis in the *cpk* mouse model of PKD can be extended to other PKD models, and additionally whether it has an effect on the liver lesion that accompanies renal cysts in ARPKD [17;25;70]. For this purpose we chose to use the *orpk* line, which is a mouse mutation that develops kidney and biliary lesions which parallel those of human patients with ARPKD [26]. We chose to use a similar dose of taxol (10 μg/g BWt. by intraperitoneal injection weekly) that was reported to be nontoxic to the animals and proved effective in decreasing the progression of renal cyst formation in *cpk* mice [55].

We maintained the *orpk* mutation on the FVB/N strain, since on this genetic background the phenotype is the most severe. *Orpk* homozygous mutants are noticeably growth retarded, and die within a few weeks after birth [26]. Since the *orpk* mutation has been characterized at the molecular level, we were able to genotype the individual animals to verify that they were homozygous for the trait.

To evaluate the effect of the taxol treatment on body weight and survival, values for life span were determined for mice of each treatment group (Fig. 1), and all animals were weighed twice weekly for control and mutant mice in each group (Fig. 2). There was no significant difference in mean life span between the mutant mice in each treatment group. The mutant mice in each group died or were sacrificed due to illness by 28 days of age except for one animal in the DMSO treatment group, which lived to 45 days of age. All control mice lived for the full 50 days with no adverse effects from the taxol or DMSO treatments. There was no significant difference in the weight curves of the control mice of treatment Group 1 and 2, indicating that taxol had no effect on growth in these animals.

To evaluate kidney tubule function, we calculated the Uosm:Sosm ratio , which is the parameter that best correlates with the decreased ability of the kidney to function as the cystic disease progresses[27]. We found no significant difference between the treatment groups with respect to the Uosm:Sosm ratio (Fig. 3). The latter result indicated that the compromised renal concentrating ability was not corrected by treatment with taxol. Since the *orpk* mutant mice have normal serum creatinine and urea nitrogen concentrations, these parameters were not measured.

Histological examination of the kidney lesions showed no difference in the severity between the treatment groups (Fig. 4), and morphometric analysis of the renal cysts confirmed that there was no difference in the progression of the renal lesions between the treatment groups (Table 1). Lectin staining of the

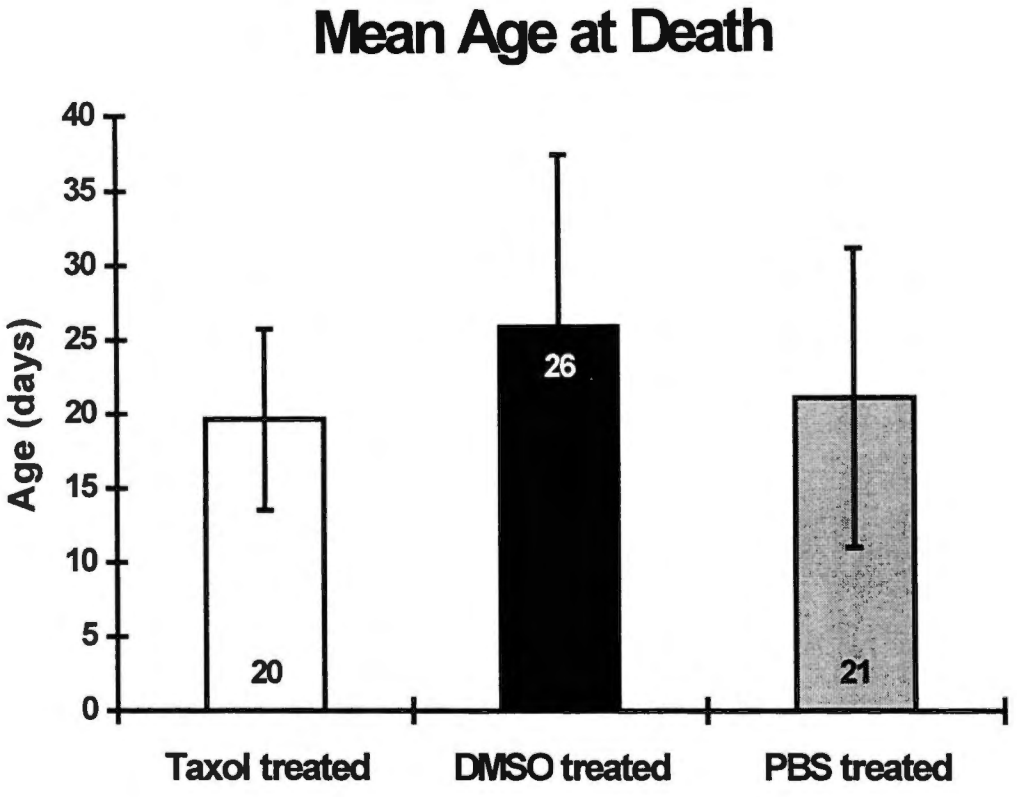

Figure 1. Mean age at death for ten *orpk* mutant mice in each treatment group. Mean values are presented within each column and bars indicate the standard deviation of the mean. Source: Sommardahl CS, Woychik RP, Sweeney WE, Avner ED, Wilkinson JE: Efficacy of taxol in the *orpk* model of polycystic kidney disease. Pediatr.Nephrol. 11:728-733, 1997.

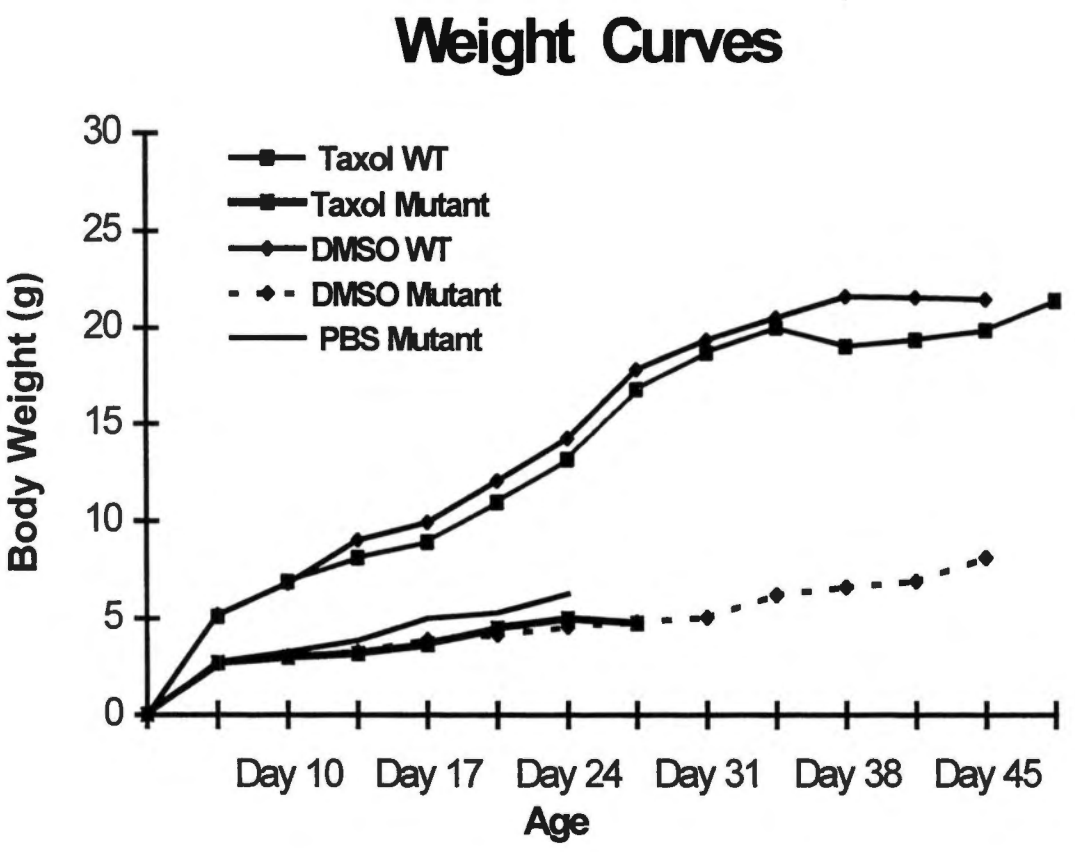

Figure 2. Mean body weight curves during the study for 10 wild-type (*WT*) control animals in the taxol- and DMSO-treated groups and the 10 mutant animals in the taxol-, DMSO-, and PBS-treated groups. Source: Sommardahl CS, Woychik RP, Sweeney WE, Avner ED, Wilkinson JE: Efficacy of taxol in the *orpk* model of polycystic kidney disease. Pediatr.Nephrol. 11:728-733, 1997.

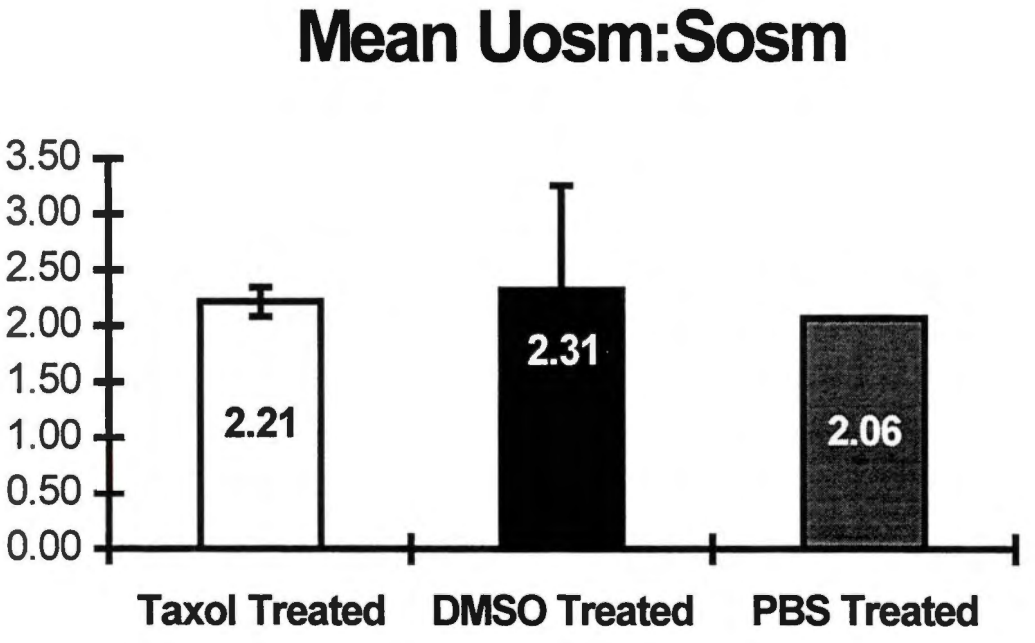

Figure 3. Mean urine to serum osmolality ratio for *orpk* mutant mice in each treatment group. Mean values are presented within the column and bars indicate the standard deviation of the mean. (Taxol-treated *orpk* mutants *n* = 3, DMSO-treated *orpk* mutants *n* = 3, PBS-treated *orpk* mutants *n*= 2). Source: Sommardahl CS, Woychik RP, Sweeney WE, Avner ED, Wilkinson JE: Efficacy of taxol in the *orpk* model of polycystic kidney disease. Pediatr.Nephrol. 11:728-733, 1997.

Figure 4. Histological sections of kidneys (hematoxylin and eosin, X10) from 28-35 day old *orpk* mutant mice from each treatment group showing the development of renal cysts. Kidney section from **(A)** taxol treated *orpk* mutant, **(B)** DMSO treated *orpk* mutant, and **(C)** PBS treated *orpk* mutant showing no difference in the severity of the renal cystic lesions between each treatment group. Source: Sommardahl CS, Woychik RP, Sweeney WE, Avner ED, Wilkinson JE: Efficacy of taxol in the *orpk* model of polycystic kidney disease. Pediatr.Nephrol. 11:728-733, 1997.

C
B
A

Table 1. Cystic index for untreated mice, and taxol-treated and dimethyl sulfoxide (DMSO)-treated control and *orpk* mutant mice calculated as the mean of the individual cyst scores. Source: Sommardahl CS, Woychik RP, Sweeney WE, Avner ED, Wilkinson JE: Efficacy of taxol in the *orpk* model of polycystic kidney disease. Pediatr.Nephrol. 11:728-733, 1997.

Treatment Group	Cystic Index
Untreated controls	0
Taxol treated controls	0
DMSO treated controls	0
Untreated mutants	4.0(0.50)
Taxol treated mutants	4.0(0.50)
DMSO treated mutants	4.25(0.57)

kidney sections also showed no difference in the progressive shift in cyst localization between the treatment groups, indicating that taxol had no effect on cystogenesis at any stage of the disease.

We also determined whether taxol has any effect on the development of the hepatic lesions that develop in the *orpk* mutants. In the FVB/N genetic background, the liver lesion in the *orpk* mutant is normally characterized by proliferation of poorly differentiated epithelial cells emanating from the portal triads that form primitive, dysplastic ductules that expand the periportal areas [26]. Histological examination of the livers of *orpk* mutant mice showed no differences in the lesions between the treatment groups (Fig. 5). We also evaluated the serum concentration of ALP and ALT, which are normally elevated in response to liver damage. Serum concentrations of ALP were markedly elevated and serum concentrations of ALT were mildly elevated in *orpk* mutant mice, and it did not appear that taxol had any affect on decreasing either parameter (Fig. 6). Serum concentrations of ALP and ALT in the control mice were within normal limits for FVB/N mice.

Finally, we determined whether taxol treatment has any effect on the targeting of the EGFR within the epithelial cells lining the renal cysts. Recent studies have focused on the role of TGF-α and EGF along with their common receptor, EGFR, in the epithelial hyperplasia in the collecting tubules and ducts. The EGFR, which is normally present only on the basolateral surface, is mistargeted to both the basolateral and apical surfaces of cystic collecting duct epithelium in PKD [71-73]. The intracellular microtubular network plays a role in receptor localization to membranes and inhibition of this function by taxol may disrupt the mislocalization seen in the cysts. Our results showed no difference in the

Figure 5. Histological sections of liver (hematoxylin and eosin, X10) from 28-35 day old *orpk* mutant mice from each treatment group showing the biliary hyperplasia/dysplasia in the periportal regions. Liver sections from **(A)** taxol treated *orpk* mutant, **(B)** DMSO treated *orpk* mutant, and **(C)** PBS treated *orpk* mutant showing no difference in the liver lesions between each group. Source: Sommardahl CS, Woychik RP, Sweeney WE, Avner ED, Wilkinson JE: Efficacy of taxol in the *orpk* model of polycystic kidney disease. Pediatr.Nephrol. 11:728-733, 1997.

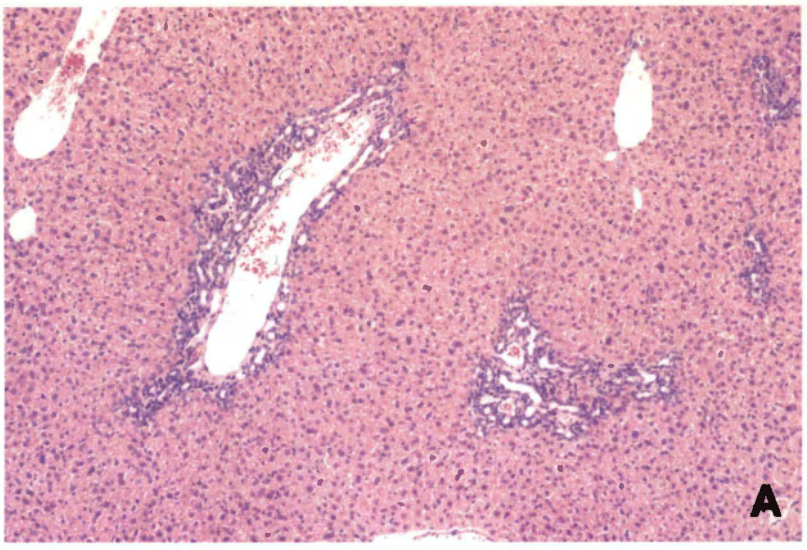
A

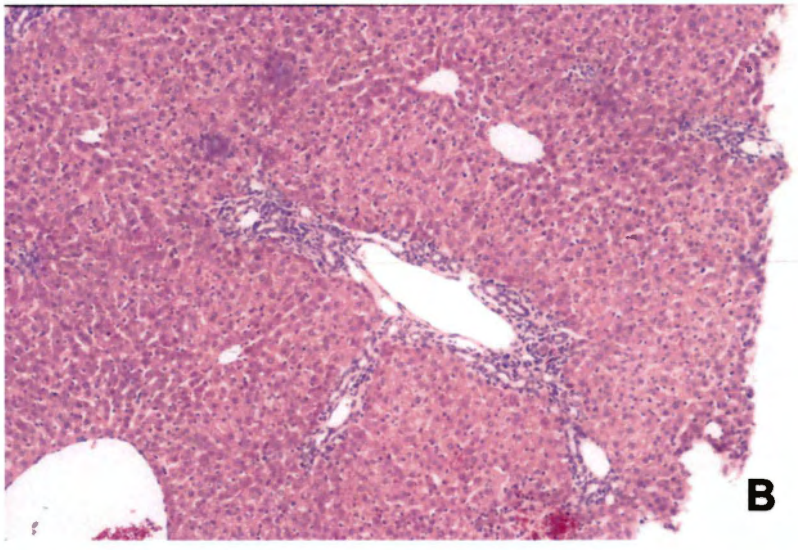
B

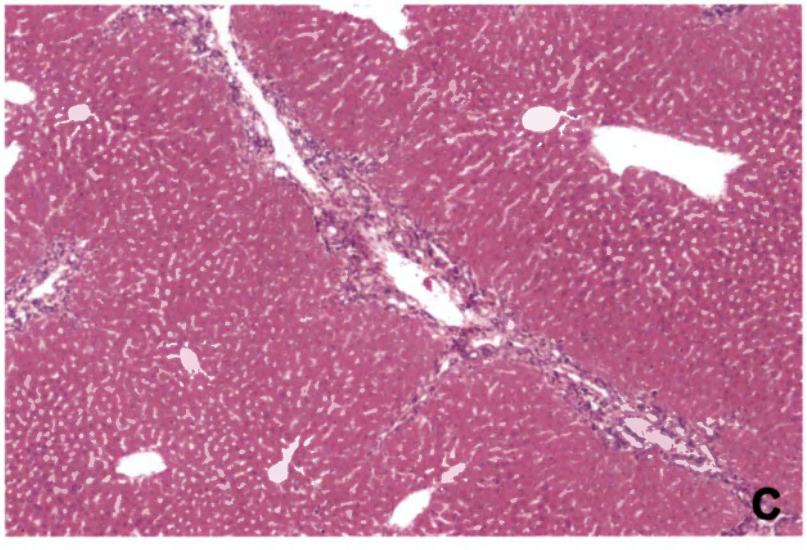
C

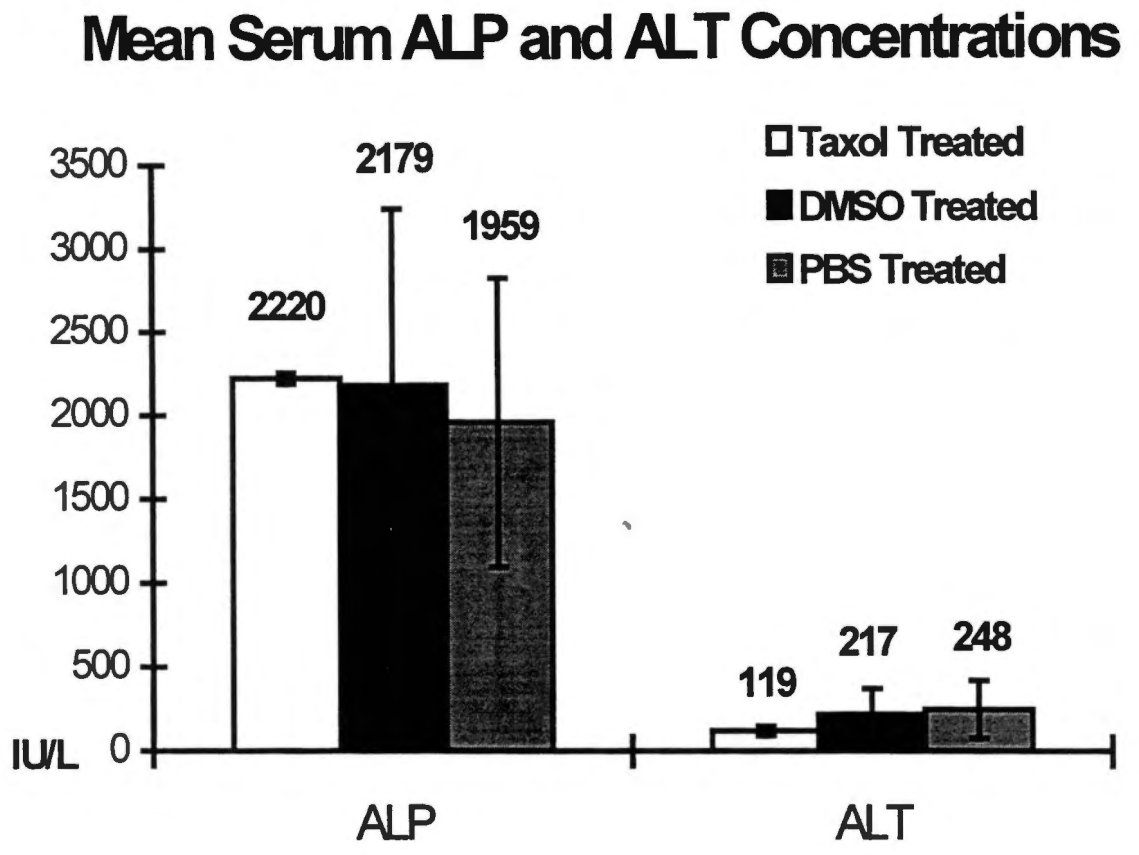

Figure 6. Mean values for serum concentrations of alkaline phosphatase (ALP) and alanine transaminase (ALT) for *orpk* mutant mice in each treatment group. Mean values are presented at the top of each column and bars indicate the standard deviation of the mean. (Taxol-treated *orpk* mutants *n* = 3, DMSO-treated *orpk* mutants *n* = 3, PBS-treated *orpk* mutants *n* = 2) Source: Sommardahl CS, Woychik RP, Sweeney WE, Avner ED, Wilkinson JE: Efficacy of taxol in the *orpk* model of polycystic kidney disease. Pediatr.Nephrol. 11:728-733, 1997.

mislocalization of the EGFR with taxol treatment (Fig. 7). This result indicates that the mislocalization occurs independent of microtubular function.

Discussion

The availability of a drug that has the potential to control the formation of renal cysts would revolutionize the treatment of PKD. In experiments with the *cpk* mouse model for PKD, Woo *et al* previously determined that taxol at a dose of 150 μg injected into an affected mouse on a weekly basis decreased the progression of renal cystogenesis and had only minimal toxicity to the animal [55]. It remained to be determined whether taxol treatment is applicable to other heritable forms of PKD that are initiated by different mutations. This is important since the predominant forms of human PKD are not initiated by the same genetic defect that triggers the disease in the *cpk* mouse mutant [10;17]. Here we describe experiments with the *orpk* mouse mutation, which causes a form of recessive PKD that closely resembles the disease progression in humans with ARPKD [26]. Taxol has no effect on the disease in the *orpk* mutants when given at the dose that was effective in the *cpk* model. In all evaluated parameters, including body weight, survival, and hepatorenal histology, there was no improvement with taxol treatment. Therefore, we conclude that taxol treatment is not effective in this particular model of PKD.

This report tests taxol under treatment conditions determined to be effective in another murine model of PKD [55]. The dose utilized (10μg/g) has been shown to have beneficial effects in the *cpk* mutant in unpublished studies by ourselves

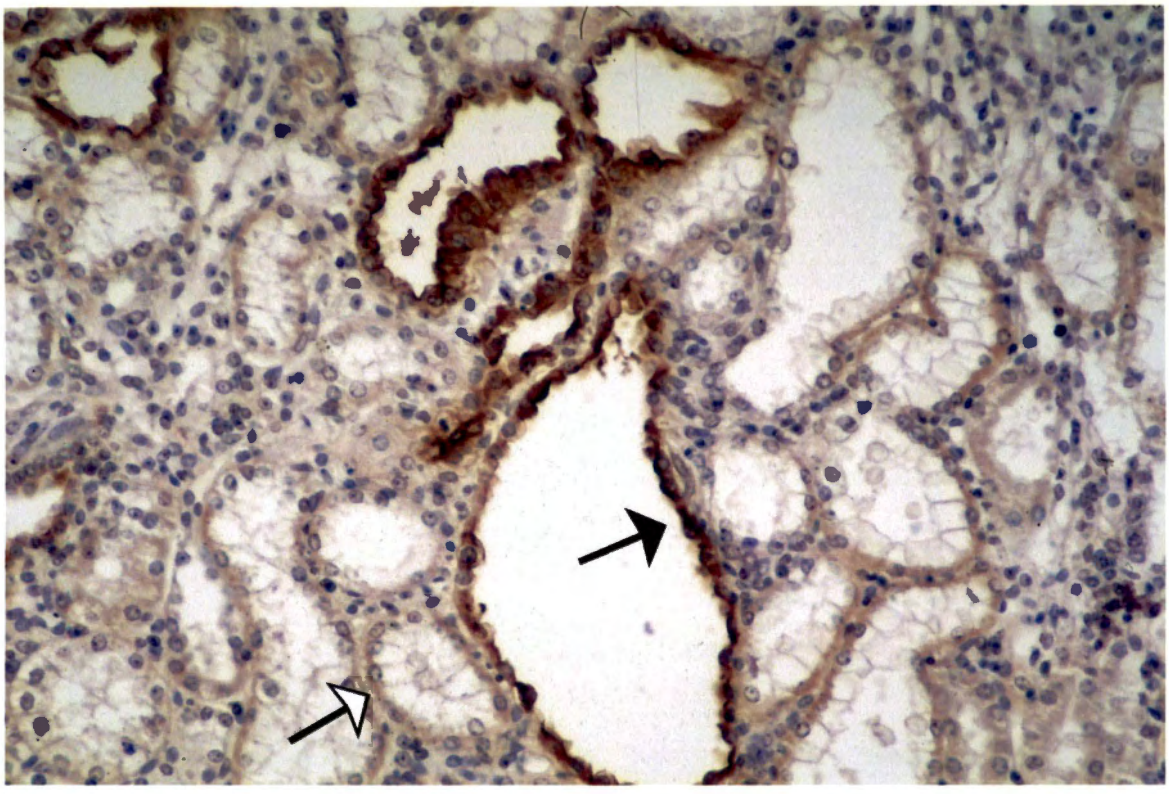

Figure 7. Histological sections of a kidney (132X) showing the immunohistological localization of the EGFR in the taxol treated orpk mutant with the EGFR localization to both the apical (solid arrow) and basolateral surfaces in cystic epithelium, but only to the basolateral surface in noncystic tubules (open arrow).

and Woo et al. (personal communication). The *orpk* mutation is on the FVB/N genetic background, while the *cpk* mutation is on a C57BL/6 genetic background, raising the possibility that genetic background may have an influence on the effectiveness of taxol as a therapeutic agent. Genetic background can influence the expressivity of genetic traits. In fact, modifier genes on chromosome 1 and chromosome 10 for the *jck* mouse model for ADPKD have already been mapped [74]. These modifying loci mediate the severity of PKD in the *jck* mouse. Thus, some of the variability in PKD expressivity in the human population may be accounted for by genetic background. Additional experiments with the *orpk* mutation on the C57BL/6 and other backgrounds will address this possibility.

Provided that genetic background and dose are not contributing factors in the lack of effectiveness of taxol, it is possible that the *cpk* mutation is fundamentally different than the *orpk* mutation at the molecular and cellular level. Although both forms of PKD exhibit a localized proliferation of epithelial cells and mistargeting of the EGFR [27;71;72], the initiating event is different since the two mutations map to different chromosomes [17;26]. Also, the disease conditions have a different progression of the renal pathology, and different multiorgan histopathology. In the *cpk* mutant mouse, the collecting duct cysts progress to cause gross enlargement of the kidneys, and the mice die of uremia within 4-5 weeks of age [17]. In contrast, the collecting duct cysts in the *orpk* mutant mice rarely cause enlargement of the kidneys and the mice do not develop uremia [26]. In the *cpk* model, the microtubule network may play a role in the cystogenesis since taxol interferes specifically with microtubule functions [39]. This may not be the case for the *orpk* mutant line. For this reason it will be important to test other mutants to determine whether they respond to taxol

treatment. Of particular interest will be targeted mutants in the mouse genes for ADPKD once these mouse strains become available.

Taxol also failed to alter the proliferation and dedifferentiation of the biliary ductules within the livers of *orpk* mutant mice. These abnormalities in the intrahepatic biliary tract are a constant and prominent feature of both *orpk* mutant mice and humans with ARPKD, but not *cpk* mice. The liver lesions become progressively more severe with age in ARPKD patients, and portal hypertension, hepatosplenomegaly, bleeding esophageal varices, and ascending cholangitis are common complications [70;75]. Therefore, even if a drug is not effective against the renal cysts, it may still have potential therapeutic value if it is active in ameliorating the liver lesion. This is not the case with taxol in this study.

The development of pharmaceuticals that are effective in the treatment of PKD will undoubtedly follow from a better understanding of the cellular and molecular events that trigger the formation of renal cysts. Knowing specifically which molecules are not functioning properly can be useful for the development of designer drugs that target a specific defect. For example, we recently have bred animals carrying the *orpk* mutation to *waved-2* mice that harbor a mutation in the EGFR that causes a decrease to about 10% of the normal level of tyrosine kinase activity [54]. Double mutant (*orpk/waved-2)* animals show a significant impairment in renal cyst formation revealing an *in vivo* role for the EGFR pathway in renal cyst formation in PKD. In this case, it may be possible to identify a compound that will specifically block the tyrosine kinase activity of the mistargeted EGFR on the apical surface of the collecting duct. These and other experiments should provide new insights into the development of unique therapies for human PKD.

III. PHENOTYPIC VARIATIONS OF THE *ORPK* MUTATION ON THE C3H GENETIC BACKGROUND

Introduction

In both ADPKD and ARPKD in humans, the variable expressivity of the phenotype with respect to disease progression and extrarenal manifestations is remarkable. This variability is in part due to genetic heterogeneity due to mutations in distinct genes giving rise to PKD. However, marked variability in clinical disease has been reported between kindred that probably have the same mutation predisposing them to PKD indicating that other genetic and environmental factors are likely to affect the manifestation of the phenotype [76]. Effects of genetic background have also been reported in mouse models of PKD in respect to disease severity [26;74;77;78].

To better evaluate how genetic background might influence the expressivity of the *orpk* phenotype, we have bred the *orpk*-FVB/N (*orpk*-F) animals onto the C3HeB/FeJLe background. We have made the mutant locus congenic on the C3HeB/FeJLe background (*orpk*-C3H line). Congenic *orpk*-C3H (*orpk*-C) mutant mice have a much less severe phenotype. Initial experiments clearly showed that these animals live much longer (weeks to months vs. days to weeks), develop renal cysts at a slower rate, and have a less aggressive liver lesion[26]. Here, I describe the major phenotypic variations of the *orpk* mutation on the FVB/N and C3HeB/FEJLe genetic backgrounds.

Materials and Methods

Mice

The *orpk*-F mouse model was generated as part of a large-scale insertional mutagenesis program at the Oak Ridge National Laboratory. Transgenic mice were generated on the FVB/N genetic background following standard pronuclear injection protocols [79]. The transgene was made congenic on the C3HeB/FEJLe (C3H) genetic background by breeding *orpk*-F mice hemizygous for the *orpk* locus to wild-type C3H animals. The hemizygous offspring were subsequently backcrossed to wild-type C3H animals and this was continued for 9 generations. All animals were handled in accordance with National Institute of Health guidelines.

Genotyping of animals

Genotyping of animals for the *orpk* locus was performed by polymerase chain reaction (PCR) analysis on DNA isolated from tail biopsies using previously described conditions [28]. The sequence of the primers for *orpk* genotyping are RW450-5′ ATGCACAAAGTTAGCTCTGC 3′,
RW451-5′ GGATCCAGCAATACCTCTCC 3′, and
RW452-5′CAGGCCATGGATCCAACTCT 3′. RW450 is located in the genomic sequence just 5′ to where the transgene integration occurred in the mutant animals and will thus serve as a forward primer for both mutant and wild type Tg737 alleles. RW451 is a reverse primer located at the 5′ end of the transgene and will produce a 340-bp fragment corresponding to the mutant allele. RW452

is a reverse primer generated to a genomic sequence that is deleted in *orpk* mutant animals as a result of the transgene integration and produces a 270-bp PCR fragment corresponding to the wild-type allele.

Histological analysis of renal, hepatic, and pancreatic tissues

The kidney, liver, and pancreas from *orpk*-C and *orpk*-F mutant animals were fixed in 10% buffered formalin and then processed by paraffin wax embedding. Sections (5 to 8 μm) were cut and attached to glass slides and were then dewaxed and stained with trichrome and/or counterstained with hematoxylin and eosin.

Serum and urine analysis

Blood was collected from metafane-anesthetized mutant animals by retro-orbital sinus puncture or at necropsy via cardiac puncture. Urine was collected from mutant animals by a free-catch method on cellophane. Serum was separated in microtainer tubes (Becton Dickinson, Rutherford, NJ) following the manufacturer's instructions. Serum concentrations of alkaline phosphatase (ALP) and bile acids were measured to assess liver damage and function respectively. Urine specific gravity and urine osmolality were measured, and the urine osmolality to serum osmolality ratio was calculated to assess renal concentrating ability. An automated biochemical analyzer (Spectrum, Irving, TX) analyzed serum samples. Serum and urine osmolality were measured using a vapor pressure osmometer (Wescor, Logan, UT).

Morphometric analysis

Hematoxylin and eosin stained histological sections of kidney from 10 *orpk*-F and 10 *orpk*-C mice were used for morphometric analysis of the kidney lesion. The percentage of the total area of kidney that is cystic was measured using a computerized imaging system connected to a videoscope (Bioquant, Nashville, TN). A cross-section and a longitudinal section of kidney were measured from each animal and the cystic percentages of these two sections were summed to obtain the total percentage of cystic kidney.

Results

Kidney

In the kidneys of the *orpk*-F mutants, initial mild, multifocal microscopic dilation of the proximal tubules is followed rapidly by marked dilation and cyst formation to the collecting tubules [26]. By postnatal day seven, cystic lesions were detected in collecting tubules, and a progressive shift in cyst localization from the proximal tubules to the collecting ducts was characteristic of all subsequent developmental stages [26]. The kidney lesions are morphologically similar in the *orpk*-C mutant mice, but they develop renal cysts at a slower rate and have fewer cysts at all stages of cyst development (Fig. 8). Proximal tubular cysts were not detected until 15-20 days of age. The progression shift in cyst localization from proximal tubules to collecting ducts occurs and the renal cysts are all localized to collecting tubules by 70 days of age. Morphometric

Figure 8. Histological sections of the kidneys (hematoxylin and eosin, X10) from a 20 day old *orpk*-F mutant (A), and a 28 day old *orpk*-C mutant (B). In contrast to the renal histology in the *orpk*-C mutants, large renal cysts are detectable in the *orpk*-F mutants at this age.

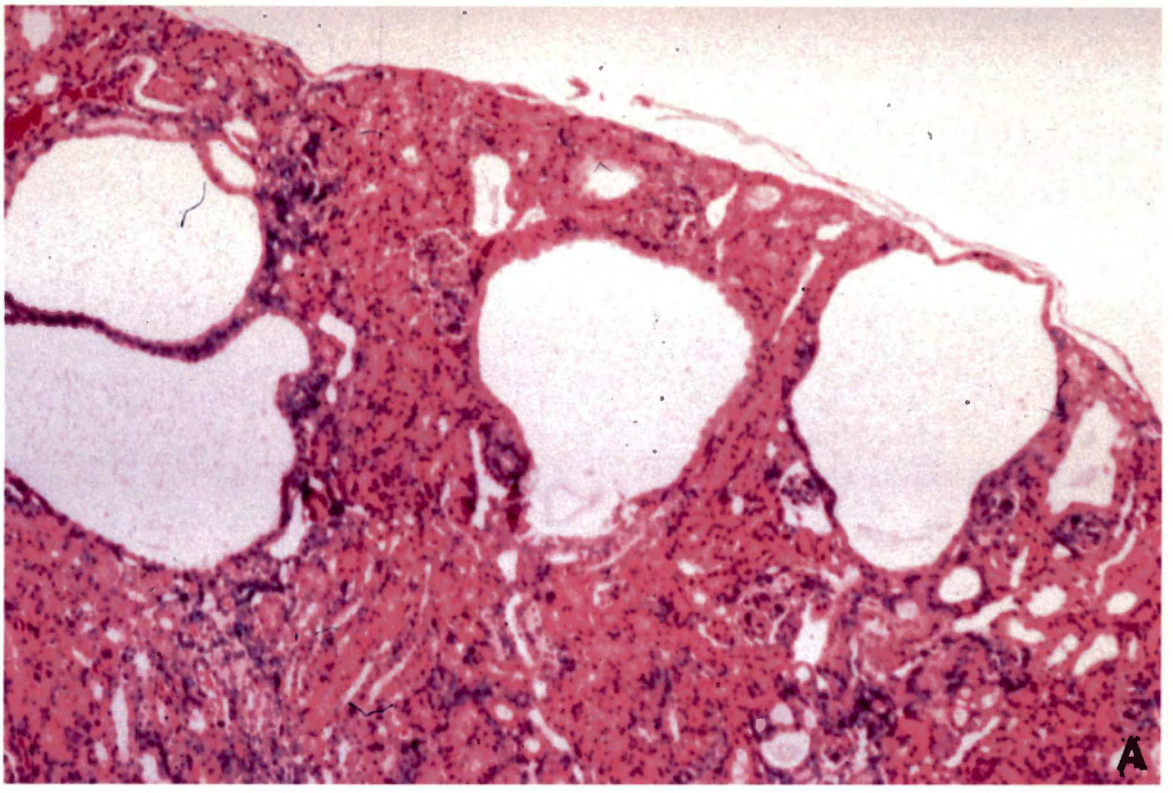
A

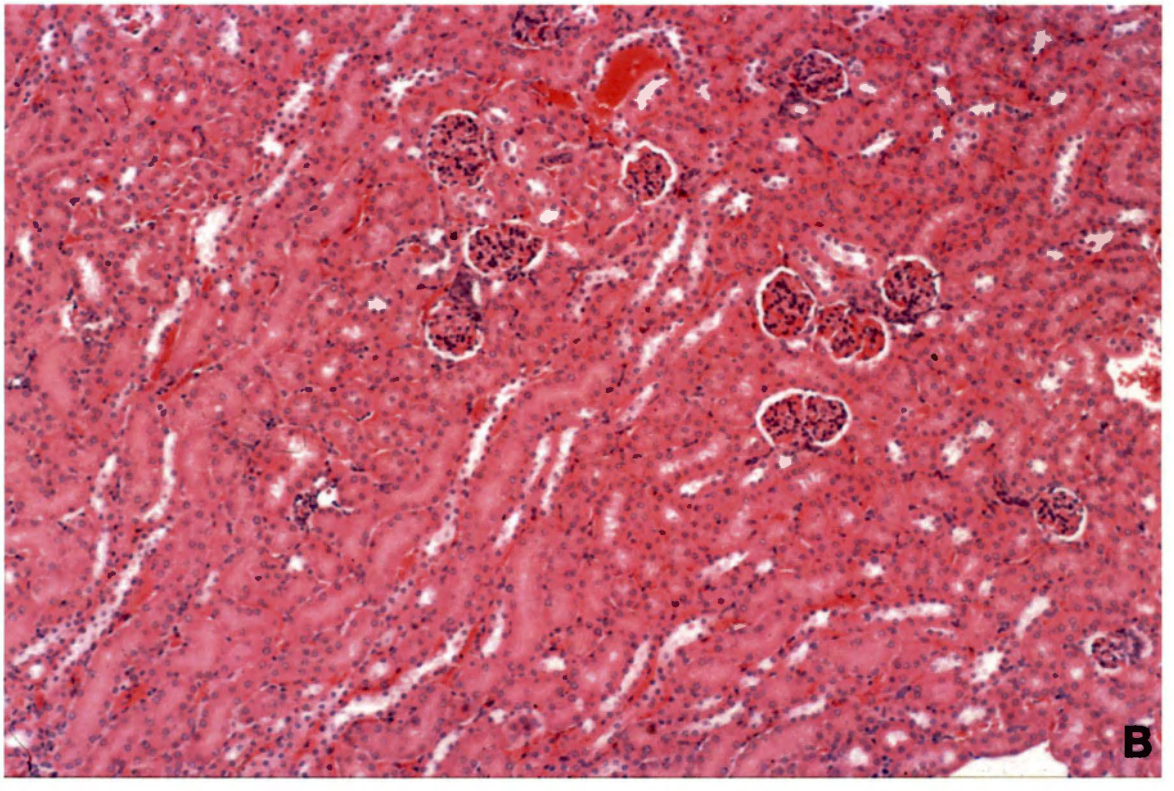
B

analysis of kidney sections from 20-30 day old *orpk*-F and *orpk*-C mutant animals showed a marked difference in the percentage of the total kidney area that was cystic. The mean values were 18.03 % and 0.58 % for the *orpk*-F and *orpk*-C mutants, respectively.

Liver

The liver lesions in the *orpk*-F mutant animals are characterized by the proliferation of poorly differentiated epithelial cells emanating from the portal triads and form primitive, dysplastic, tortuous ductules that expand the portal periportal areas (Fig. 9A). These cells can ultimately disrupt the limiting plate, isolate individual hepatocytes, and can give rise to anastomosing tortuous bile ductules in the end-stage diseased liver [26;28]. The liver abnormality is first observed in *orpk*-F mutants at postnatal day 5 with an excess of bile ductular structures and proliferation of nonparenchymal epithelial cells (oval cells) centered on the portal triad area. The proliferating oval cells expand the portal triad area and move outward from the portal triad into the periportal area as the mice mature [28]. There is very little portal fibrosis observed within these lesions. The liver lesions in the *orpk*-C mutant animals are not as diffuse and are characterized by multifocal biliary hyperplasia, dysplasia, and portal fibrosis isolated to the portal triad regions (Fig. 9B). These features more closely resemble the liver lesion in human ARPKD. The most striking feature of the *orpk*-C phenotype is the formation of excess biliary ductules secondary to biliary hyperplasia that expand the portal triad area. The lesions are seen in the first week postnatal and begin as mild biliary hyperplasia and dysplastic duct formation. As the mice mature, the biliary ducts continue to proliferate forming

Figure 9. Histological sections of the liver (hematoxylin and eosin, X10) from a 24 day old *orpk*-F mutant (A), and a 20 day old *orpk*-C mutant (B). The liver lesion is more extensive in the *orpk*-F mutants with hyperplasia of oval cells (arrows in A) expanding the portal triad area into the periportal space. The liver lesions in the *orpk*-C mutant animals are not as diffuse and are characterized by multifocal biliary hyperplasia, dysplasia, and portal fibrosis isolated to the portal triad regions (arrows in B).

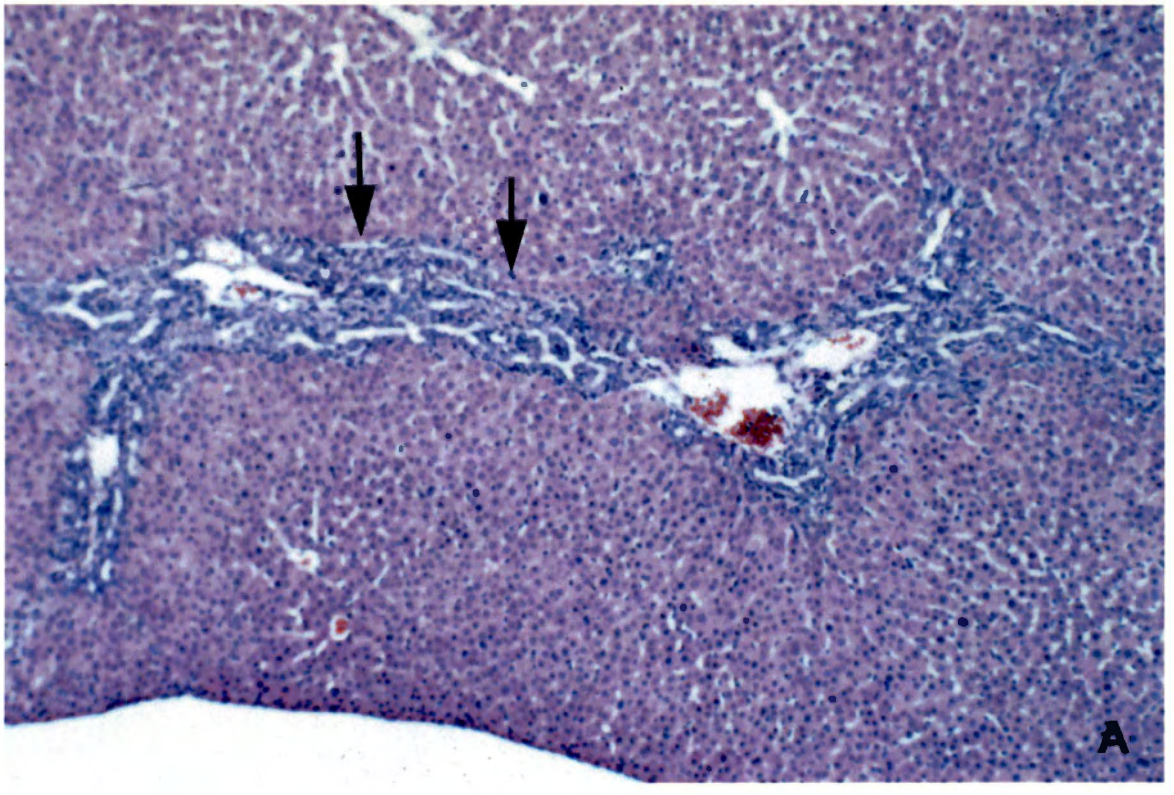
A

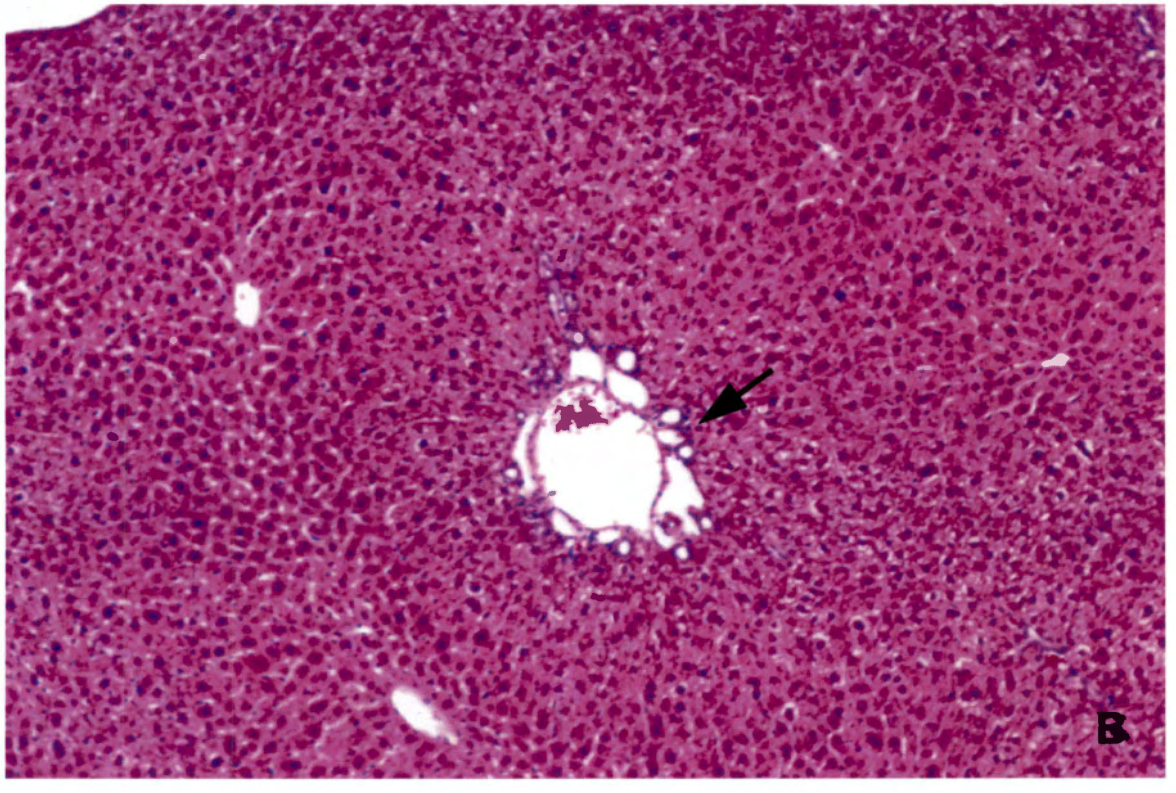
B

multifocal areas of biliary hyperplasia and dysplasia centered on the periportal area. There is a decrease in the presence of the proliferating nonparenchymal cells seen in the *orpk*-F mutant animals. However, there is a greater degree of fibrosis present surrounding the dysplastic biliary ductules.

Pancreas

The pancreatic lesion in the *orpk*-F mutant animals begins as pancreatic ductular hyperplasia and dysplasia that disrupts the normal acinar cell architecture. The proliferating ducts become the prominent features of the pancreas as the acinar cells disappear. This disappearance of the acinar cells is felt to be secondary to apoptosis, since there is no evidence of necrosis or inflammation within the lesions. The islets of Langerhans are not affected by the ductular hyperplasia, although there appears to be fewer present in the sections examined. As the *orpk*-F matures, the normal exocrine pancreatic tissue disappears, leaving scattered islets of Langerhans within the mesenteric adipose tissue. This pancreatic lesion is highly variable between *orpk*-F mutant animals and the degree of severity seems to correlate with the survival of the mutants. The mutants that live past weaning have more exocrine pancreatic tissue present than those that die early in life. The pancreatic lesion in the *orpk*-C mutant animals also begins as a pancreatic ductular hyperplasia and dysplasia that expands into the normal acinar cell tissue. The proliferating ductules progress to form cyst structures that enlarge to form space-occupying cysts within the abdomen (Fig. 10). The developing cysts can be seen microscopically as early as 15-20 days of age and occur prominently in the cranial arm of the pancreas that lies near the greater curvature of the stomach

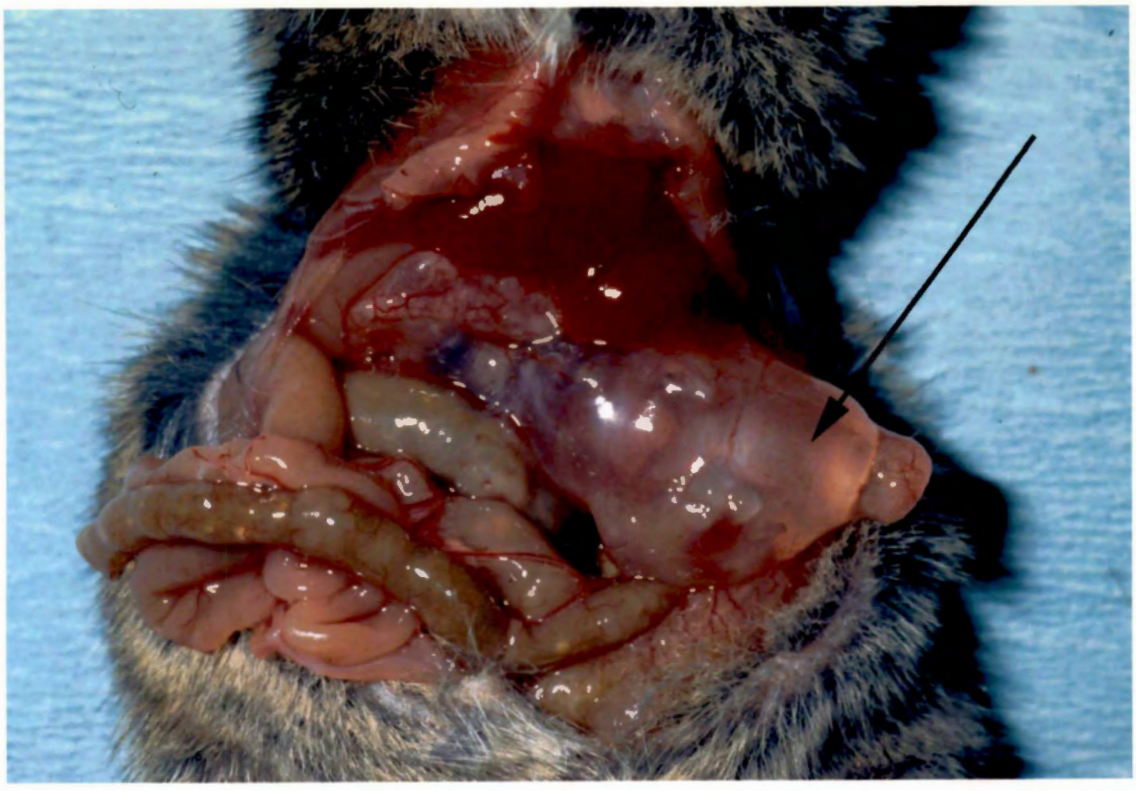

Figure 10. Gross appearance of a large pancreatic cyst (arrow) occupying the cranial abdominal area in a 90 day old orpk-C mutant.

and the spleen. The cysts are lined by a cuboidal epithelium that resembles normal pancreatic ductular epithelium and are fluid filled. The dysplastic pancreatic ductules and cysts are surrounded by extensive fibrosis and the normal acinar cell structures are reduced (Fig. 11). The islets of Langerhans are not affected by the proliferating ductules, but are crowded by the expanding cysts, as is the rest of the normal pancreatic architecture.

Serum and Urine Analysis

The *orpk*-F mutants have urine with low specific gravity and low urine: serum osmolality ratio indicating that the renal concentrating ability is compromised. Serum creatinine and urea nitrogen concentration, however, are normal in these animals. The *orpk*-C mutants retain their renal concentrating ability as measured by urine specific gravity and urine:serum osmolality (osm) ratio until late in the disease progression (Fig. 12). Serum creatinine and urea nitrogen concentrations are also within normal limits in these animals.

Serum concentration of alkaline phosphatase (ALP), a liver enzyme used as a marker of biliary abnormalities, and serum concentration of bile acids are markedly elevated in *orpk*-F mutants supporting the biliary origin of the lesions. Serum concentrations of ALP and bile acids in the o*rpk*-C mutant animals are only mildly elevated as compared to *orpk*-F mutants (Fig. 13).

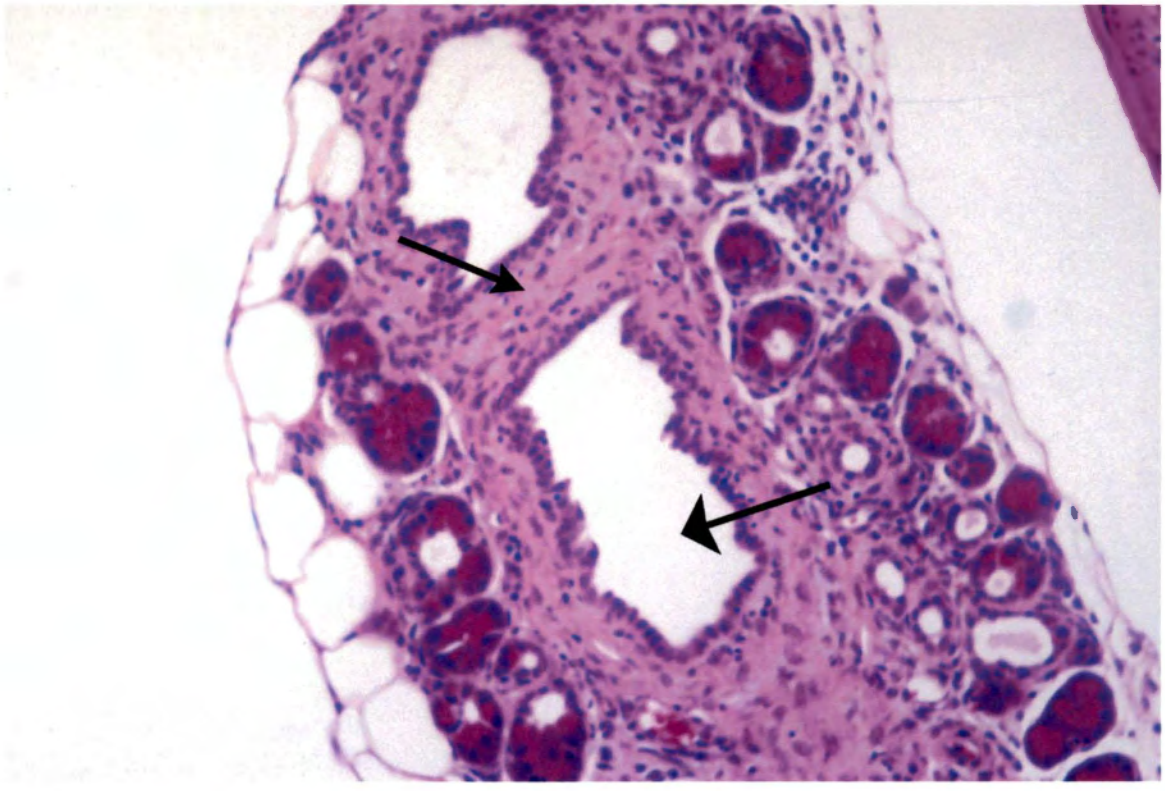

Figure 11. Histological section of the pancreas (hematoxylin and eosin, X10) from a 24 day old orpk-C mutant showing the dysplastic pancreatic ductules and cysts (large arrow) surrounded by extensive fibrosis (small arrow).

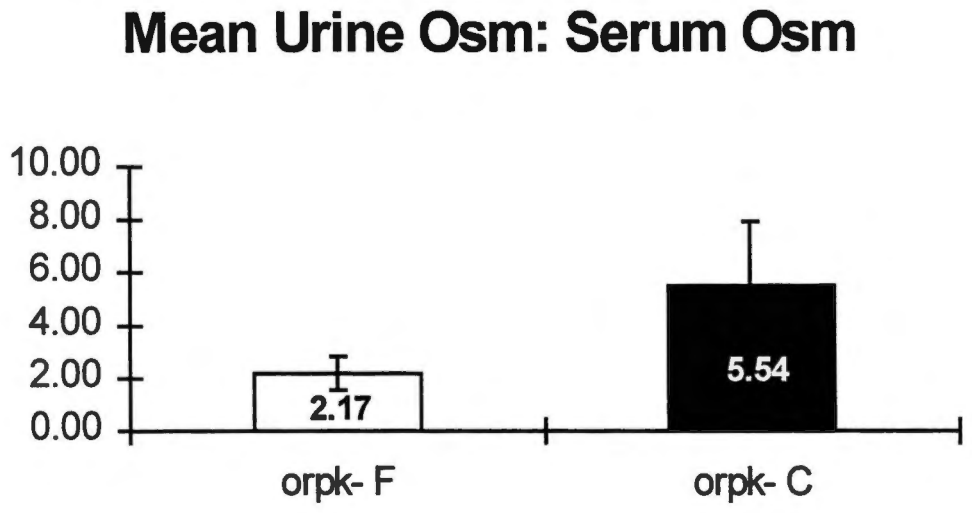

Figure 12. Renal concentrating ability was analyzed by comparing the mean urine osmolality:serum osmolality (urine osm:serum osm) ratio in the *orpk*-F mutants and the *orpk*-C mutants demonstrating a loss of concentrating ability in the *orpk*-F mutants. Mean values are presented within each column and bars indicate the standard deviation of the mean.

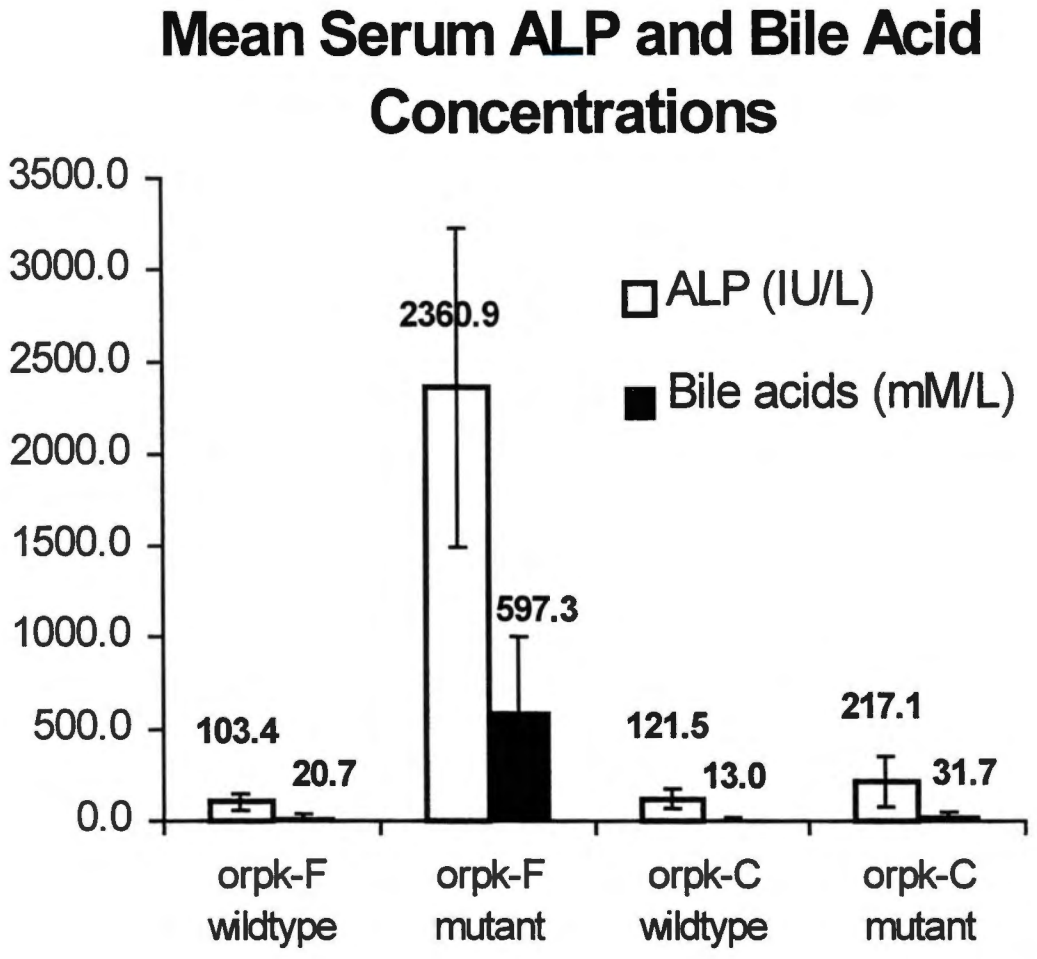

Figure 13. Mean serum alkaline phosphatase (ALP) and bile acid concentrations in *orpk*-C mice and *orpk*-F mice demonstrating the marked elevation in the *orpk*-F mutant. Mean values are presented at the top of each column and bars indicate the standard deviation of the mean.

Discussion

The major phenotypic variations of the *orpk* mutation on the FVB/N and C3H genetic backgrounds have been described. As in human ARPKD, the pathologic features of the *orpk* phenotype include a spectrum of disease with variable severity in which the primary lesions of the kidneys and liver are expressed to different degrees. In the FVB/N genetic background, the phenotype is very severe in the kidney, liver, and pancreatic lesions and the majority of the animals die within several weeks after birth. Congenic *orpk*-C mutant mice have a much less severe phenotype and survive to several months of age. This dramatic decrease in severity is evident in first generation backcross to C3H. The most striking variation in severity was in the kidney phenotype. The kidney lesions are morphologically similar in both genetic backgrounds, but the *orpk*-C mutants develop renal cysts at a slower rate and have fewer cysts at all stages of cyst development. The progressive shift from proximal tubular dilations to collecting tubule cysts is evident in both genetic backgrounds, however, the disease progression is much more rapid in the *orpk*-F mutants. The kidneys of *orpk*-C mutants do not show tubular dilations or cysts until they are 2-3 weeks of age. The renal cysts are not localized to collecting tubules until they are 2-3 months of age and end-stage renal disease is not evident until much later. These animals also retain their renal concentrating ability as measured by urine specific gravity and urine: serum osmolality ratio until late in the disease progression.

As with the renal lesion, the hepatic abnormality detected in both genetic backgrounds is similar to some degree, but the *orpk*-F mutants develop a much more severe lesion, which progresses rapidly. The common feature of the liver

phenotype in both genetic backgrounds is the biliary ductular hyperplasia and formation of numerous bile ductule- like structures. The *orpk*-F mutants also have a proliferation of an immature epithelial cell characterized as an oval cell. This proliferation expands the lesion from the portal triad into the periportal area invading the hepatic parenchyma. The proliferating oval cells eventually form-bridging lesions between portal triads causing a diffuse hepatic lesion. Conversely, the lesion in the *orpk*-C mutants remains confined to the portal triads with the formation of an excess of biliary ductular structures that expands the portal area as the lesions progress. There is a marked reduction to an absence of the proliferating oval cells in the *orpk*-C mutants, but there is a greater degree of fibrosis within the liver lesions. This difference in the cell types present in the lesions suggests a variation in the differentiation signals or response to these signals between the two genetic backgrounds when the *orpk* mutation is present. The liver lesions in the C3H background are characterized by multifocal biliary hyperplasia, dysplasia, and portal fibrosis isolated to the portal triad regions. These features more closely resemble the liver lesion in human ARPKD. The elevation in serum ALP and bile acid concentrations seen in the *orpk*-F mutants may simply be a reflection of the severity of the liver lesion in these animals compared to the *orpk*-C mutants. The elevated ALP may also be due to the proliferation of the oval cells that occurs in the *orpk*-F mutants.

The pancreatic lesion has not previously been described in the *orpk*-F mutants, and is also more severe in these animals than in the *orpk*-C mutants. The loss of normal exocrine pancreatic acinar tissue in the *orpk*-F mutants begins shortly after birth and is a major factor in their runted appearance and poor growth, since the exocrine pancreas is a key player in the digestion of

nutrients. The loss of acinar tissue in the *orpk*-C mutants is much slower occurring over several weeks, however, they develop pancreatic ductular cysts that grow into large cysts within the cranial abdominal cavity. Pancreatic cysts are uncommon in human ARPKD patients but have been reported to occur in 10% of patients with ADPKD [6]. Pancreatic cystic disease has recently been reported in a mouse model of polycystic kidney disease with a targeted mutation that disrupts the mouse homologue of PKD1, the major gene associated with ARPKD. The mice homozygous for this mutation develop pancreatic ductual dilatation during gestation and cystic enlargement of the pancreas during the perinatal period [80]. The similarity of the lesions in these two mouse models with regard to the pancreatic lesion suggests a common pathogenesis that leads to abnormal pancreatic tubular epithelial development and warrants further investigation.

The significant difference in the lesions on a different genetic background suggests the presence of important modifier genes that vary in the FVB/N and C3H genetic backgrounds. This may be also the case in human ARPKD and ADPKD, in which the severity of the phenotype and the nature of the extrarenal lesions can be quite variable. Based on the analysis of these phenotypes, the modifier genes appear to be dominant in the C3H background since this dramatic decrease in severity is evident in first generation backcross to C3H. The *orpk*-C mutants also provide a model of the extrarenal lesions of ARPKD and ADPKD that can be studied to better understand the development of the epithelial proliferation and dysgenesis in the liver and pancreas.

IV. CHROMOSOMAL LOCALIZATION OF THE MODIFIER GENES THAT INFLUENCE THE PHENOTYPIC EXPRESSION OF *ORPK* IN THE FVB/N AND C3HeB/FEJLe GENETIC BACKGROUNDS

Introduction

Significant differences in the lesions when the *orpk* mutation is on a different genetic background suggest the presence of important modifier genes that vary in the FVB/N and C3H genetic backgrounds. Effects of genetic background have also been reported in mouse models of PKD with respect to disease severity [20;74;78]. Potential modifiers affecting the severity of the cystic progression have been detected in several of these mouse models [74;81-84]. In the *pcy* mouse, whole genomic quantitative trait loci mapping identified two loci that modulated PKD progression based on kidney:body weight ratio. These loci were on chromosome 4 and 16 [84]. Using the same quantitative trait character, two loci on chromosome 4 were detected in a genome scan in the *cpk* mouse model [83]. Two regions (one on chromosome 10 and one on chromosome 1) were found to be associated with inheritance of a more severe PKD phenotype in the *jck* mouse model using kidney weight as the quantitative character in a genome scan [81]. Recently, a new mouse mutation, kat 2J, on chromosome 8, that causes late-onset PKD and anemia has been identified. Genome scans revealed two loci that affect the severity of PKD based on kidney weight, one on

chromosome 1 and another on chromosome 19 [85]. At this time, these modifier loci have not been finely mapped nor have candidate genes been identified. My aim in this study was to map the chromosomal location of the modifier genes that affect the severity of disease in the *orpk* mouse between the FVB/N and C3H genetic backgrounds.

Microsatellite DNA Variants between the FVB/N and C3H Mouse Strains

The FVB/N strain originally arose from an outbred colony of N:GP Swiss mice at the National Institute of Health (NIH). They are commonly used in the generation of transgenic animals, because the male pronucleus is easily visualized and they have good reproductive performance [86]. The use of FVB/N for genetic mapping studies is limited by the lack of information regarding DNA variant alleles between FVB/N and other inbred mouse strains. Therefore, the first step in my QTL analysis was to identify SSLP or microsatellite markers spread throughout the genome that are polymorphic between the FVB/N and C3HeB/FeJLe (C3H) strains. In a collaborative study with Dr. David Beier's laboratory at the Harvard Medical School, Boston, we have screened over 300 microsatellite markers distributed throughout the genome for polymorphism between FVB/N, C57BL/6J (BL/6), and C3H mouse strains and these results have been published [87].

Materials and methods

FVB/N, C3H, and BL/6 were obtained from The Jackson Laboratory and the Oak Ridge National Laboratory. Genomic DNA was prepared from mouse tails and amplified by PCR with primers for microsatellite markers developed at the Whitehead Institute/MIT center for Genome Research and obtained from Research Genetics (Huntsville, Ala). PCR was carried out in either of two protocols. Protocol 1 was as follows: an aliquot of 100 ng of genomic DNA was amplified in 20 µl PCR reaction containing 10 mM Tris-HCL (pH 8.0), 50 mM KCL, 1 µM of each primer, 2.0 mM $MgCl_2$, 250 µM each dNTP, and 2.5 units of Taq polymerase (Boehringer-Mannheim, Ind.). PCR reactions were overlaid with 20 µl of mineral oil (Sigma, Mo.) and amplified in a thermal cycler (Hybaid) as follows: 1 cycle 95°C for 5 min, 60°C for 2 min, and 72°C for 3 min; 30 cycles 95°C for 1 min, 60°C for 2 min, and 72°C for 3 min. A final elongation step at 72°C for 10 min followed. Protocol 2 was as follows: an aliquot of 20 ng of genomic DNA was amplified in 20 µl PCR reaction containing 22 mM Tris-HCl (pH 8.4), 55 mM KCl, 0.66 µM of each primer, 1.65 mM $MgCl_2$, 880 µM dNTPs, and 0.44 units of Taq polymerase (Gibco-BRL). PCR reactions were amplified in a thermal cycler (MJ Research) as follows: 1 cycle 95°C for 5 min; 30 cycles of 95°C for 45 s, 45-55°C for 45 s, and 72°C for 2 min and 30 s. A final elongation step at 72°C for 5 min followed. PCR products were run in 3% agarose gels. When necessary, PCR products were labeled in the presence of [α-P^{32}] dCTP (NEN), by including 0.125 µl of a stock solution (3000 Ci/mmol) in a 10-µl PCR reaction. Radiolabeled DNA products were run in denaturing polyacrylamide gels followed by an X-ray autoradiography with standard protocols [88]. Alternatively, unlabeled DNA products were run in nondenaturing polyacrylamide

gels and silver stained with standard protocols [89]. Variant alleles between the FVB/N and C3H mouse strains were analyzed with a set of 390 microsatellite markers distributed along 20 mouse chromosomes; 272 microsatellite markers were also tested between FVB/N and BL/6 mouse strains. All microsatellites were analyzed in 3% agarose gels, or polyacrylamide gels were used to score variant alleles in cases where difference in allele size was <6 bp.

Results and discussion

Of 390 markers tested between FVB/N and C3H mouse strains, 189 (48%) were variant. Of 272 markers tested between FVB/N and BL/6 mouse strains, 145 (53%) were variant. Approximately half of the variant markers were differentiable in 3% agarose gels, suggesting a difference in size of >6 bp. The results are shown in Table 2.

This rate of variant alleles reported is comparable to that found between other inbred laboratory mouse strains [65]. The results of this study provide the information required to perform the QTL analysis and will be useful for other investigators that would like to utilize the FVB/N inbred strain for genetic mapping studies.

Table 2. Variant alleles between FVB/N and the mouse strains C3He/FeJLe and C57BL/6J. C, C3He/FeJLe; B, C57BL/6J; cM, map position in centimorgans; -, no detected variant allele; >, variant allele size < 6 bp; >>, variant allele size ≥ 6 bp; ♦, PCR products were tested in polyacrylamide gels.

1	Cm	C	B	Pg
D1Mit1	8.7	-	-	
D1Mit2	9.0	-	-	
D1Mit3	11.0	-	F>>B	♦
D1Mit7	41.0	C>>F	-	♦
D1Mit10	56.6	C>F		
D1Mit11	58.7	-		♦
D1Mit16	87.2	-		
D1Mit17	106.3	C>F	F>B	♦
D1Mit19	36.9	F>>C		
D1Mit20	18.5	C>F		♦
D1Mit23	41.0	-		
D1Mit24	41.0	-	-	
D1Mit30	70.0	F>>C	F>>B	♦
D1Mit33	81.6	F>C		
D1Mit36	92.3	-	F>B	
D1Mit42	78.0	-	-	
D1Mit56	106.1	-		♦
D1Mit57	87.8	F>>C		♦
D1Mit62	100.5	-	-	
D1Mit64	5.0	F>>C		
D1Mit70	17.8	-	-	
D1Mit73	23.6	-	-	
D1Mit76	32.8	-	F>>B	
D1Mit80	52.0	-	B>>F	♦
D1Mit90	66.7	-	-	
D1Mit102	73.0	-	F>B	
D1Mit104	79.0	-	-	
D1Mit150	100.0	F>>C		♦
D1Mit155	112.0	-	B>>F	
D1Mit201	79.0	F>C		
D1Mit209	106.1	-	B>F	
D1Mit273	102.5	-	-	
D1Mit303	34.8	-	B>F	♦
D1Mit362	106.3	C>>F		
D1Mit403	100.0	C>>F		
D1Mit426	101.0	-		

2				
D2Mit1	1.0	F>>C	F>B	♦
D2Mit2	4.0	F>C		
D2Mit5	5.0	-	-	
D2Mit21	80.0	-	-	
D2Mit42	53.0	C>>F	B>>F	
D2Mit48	87.0	F>C	B>>F	♦
D2Mit50	96.0	-		
D2Mit52	99.0	-	-	
D2Mit53	84.2	C>F	-	♦
D2Mit55	91.0	-	-	
D2Mit57	82.0	-		
D2Mit61	34.0	-	B>F	♦
D2Mit74	107.0	F>C	F>B	♦
D2Mit149		-	-	♦
D2Mit194	81.0	F>C		♦
D2Mit266	98.4	C>F		♦
D2Mit274	52.5	C>F		
D2Mit285	72.1	C>F		♦
D2Mit312	2.2	-		
D2Mit323	31.7	F>>C		

Table 2 (continued)

3				
D3Mit10	49.7	F>>C	-	♦
D3Mit12	49.2	-	-	
D3Mit16	66.2	-	B>F	♦
D3Mit17	71.8	C>F	B>>F	♦
D3Mit19	87.6	-	F>B	♦
D3Mit21	14.2	-		
D3Mit28	45.2	-	-	
D3Mit32	80.2	C>F	-	♦
D3Mit42	58.8	F>C		
D3Mit46	13.8	C>>F	B>F	♦
D3Mit49	41.0	-	B>>F	♦
D3Mit54	4.6	-	-	
D3Mit59	84.1	C>F	B>F	♦
D3Mit62	4.6	-		
D3Mit63	22.0	-	F>B	♦
D3Mit83	65.2	-	-	
D3Mit86	76.2	-		
D3Mit89	86.1	-		
D3Mit90	4.6	C>F		
D3Mit97	39.7	C>F	-	♦
D3Mit103	51.1	-	-	
D3Mit116	84.9	-	F>>B	
D3Mit147	79.4	C>F		
D3Mit149	2.4	-		
D3Mit164	2.4	-	B>>F	
D3Mit203	11.2	F>C		
D3Mit230	38.3	F>C		
D3Nds2	64.1	-	-	

4				
D4Mit5	13.6	-	-	
D4Mit9	44.5	C>>F		
D4Mit12	55.6	-	B>>F	
D4Mit13	71.0	-		
D4Mit16	60.0	-		
D4Mit18	4.4	-	-	
D4Mit26		F>C	-	♦
D4Mit27	42.0	F>>C	-	♦
D4Mit31	47.5	F>>C	-	
D4Mit37	52.6	-	B>F	
D4Mit42	81.0	-	B>>F	
D4Mit54	65.1	F>C	F>>B	♦
D4Mit57	49.5	-	F>B	♦
D4Mit66	71.3	-	-	
D4Mit67	65.4	-		
D4Mit68	65.4	-		
D4Mit69	65.4	-		
D4Mit71	61.8	-	B>F	
D4Mit148	66.0	-	F>B	
D4Mit149	5.2	C>>F		
D4Mit158	65.4	-	B>>F	
D4Mit170	66.4	-	F>B	
D4Mit178	35.5	C>F		♦
D4Mit190	76.5	F>>C		
5				
D5Mit5	36.0	-	-	
D5Mit24	60.0	-	F>>B	
D5Mit25	61.0	C>F	B>F	♦
D5Mit43	90.0	F>>C	F>>B	
D5Mit48	0.0	C>F	B>F	♦
D5Mit70	1.0	-		
D5Mit93	54.0	C>>F	-	♦
D5Mit99	84.0	-	F>B	♦
D5Mit161	70.0	-	F>B	♦
D5Mit169	95.0	-		
D5Mit233	29.0	-	F>>B	♦
D5Mit239	56.0	-		
D5Mit267	24.0	-		
D5Mit292	84.0	C>>F		

Table 2 (continued)

6				
D6Mit1	3.0	C>>F	-	♦
D6Mit9	36.5	-		
D6Mit14	72.0	F>>C	F>B	♦
D6Mit15	77.5	C>>F		
D6Mit31	38.5	C>>F		
D6Mit32	38.5	C>>F	-	
D6Mit50	3.0	-	B>F	♦
D6Mit55	49.5	-	-	
D6Mit74	20.5	-	B>>F	
D6Mit86	0.0	-	B>F	♦
D6Mit116	6.0	-	-	♦
D6Mit131	37.0	-	B>F	♦
D6Mit138	5.0	-		
D6Mit149	46.5	C>F		
D6Mit188		-	F>B	
D6Mit261		-	B>F	
7				
D7Mit12	66.0	-		
D7Mit21	0.5	C>F	-	♦
D7Mit32	46.4	-		
D7Mit47	72.4	-		
D7Mit57	4.0	C>>F	B>>F	♦
D7Mit76	3.4	C>>F		
D7Mit89	27.0	C>>F		
D7Mit93	37.0	C>>F		
D7Mit109	66.0	-		
D7Mit250	37.0	C>F		
D7Mit259	72.4	C>F		
D7Nds4	72.4	F>>C	-	♦
8				
D8Mit3	10.5	-		
D8Mit4	14.0	-	F>>B	
D8Mit13	67.0	-		
D8Mit16	8.0	F>>C		♦
D8Mit24	18.0	C>F	F>B	♦
D8Mit25	32.0	C>>F	-	♦
D8Mit33	45.0	F>>C	-	♦
D8Mit42	71.5	F>>C	-	♦
D8Mit56	72.0	C>F	-	♦
D8Mit58	1.0	-	-	♦
D8Mit182	45.0	-	-	♦
D8Mit190	21.0	-	B>>F	♦
D8Mit191	21.0	F>>C		
D8Mit215	59.0	F>>C	B>>F	
D8Mit227	24.0	-		
D8Mit245	73.0	C>F		♦
D8Mit248	43.0	C>>F		

9				
D9Mit2	17.0	C>F	-	♦
D9Mit8	42.0	F>C		
D9Mit11	48.0	C>>F		
D9Mit12	55.0	F>C		
D9Mit15	61.0	C>>F	B>>F	♦
D9Mit18	71.0	-	F>>B	
D9Mit19	71.0	-		
D9Mit35	52.0	-		
D9Mit37	61.0	-		
D9Mit42	8.0	-		
D9Mit43	4.0	F>>C		
D9Mit45	24.0	C>>F	-	
D9Mit49	33.9	-		
D9Mit52	72.0	-	-	
D9Mit57	4.0	C>>F		
D9Mit82	74.0	-	F>B	♦
D9Mit90	9.0	F>C	-	♦
D9Mit182		-	F>B	♦
D9Mit196	48.0	F>C		
D9Mit205	18.0	F>C		
D9Mit207	33.0	-		
D9Mit212		-	F>B	♦
D9Mit229		C>>F	F>B	♦
D9Mit248	31.0	C>F		♦
10				
D10Mit3	19.0	F>C	B>>F	♦
D10Mit10	49.0	-	B>>F	♦
D10Mit11	49.0	-	B>>F	♦
D10Mit14	63.0	-	-	
D10Mit19	19.0	-	-	
D10Mit20	30.0	F>C	-	
D10Mit28	2.0	F>>C	F>>B	
D10Mit32	36.0	-	-	
D10Mit35	67.0	-	-	
D10Mit51	7.0	-	F>>B	
D10Mit73	60.0	-	-	
D10Mit80	2.0	F>>C	B>F	♦
D10Mit95	49.0	-	B>>F	
D10Mit102	67.0	-	-	
D10Mit103	68.0	C>F		
D10Mit115	37.0	C>>F	-	♦
D10Mit123	2.0	C>F		
D10Mit180	62.5	C>>F	-	♦
D10Mit198	37.0	C>>F	B>>F	
D10Mit233	61.0	-	B>>F	♦
D10Mit241	38.0	-	-	
D10Mit267	65.0	F>>C	F>>B	
D10Nds1	4.0	C>>F	F>B	

Table 2 (continued)

11				
D11Mit2	2.0	C>>F	F>B	♦
D11Mit4	37.0	F>C	-	♦
D11Mit12	71.0	C>F	-	♦
D11Mit14	59.0	C>F	-	♦
D11Mit15	40.0	-	-	
D11Mit20	20.0	C>>F	F>>B	♦
D11Mit30	40.0	-	F>B	
D11Mit34	46.0	F>C	-	♦
D11Mit36	47.0	C>F	B>F	♦
D11Mit38	49.0	-	F>>B	
D11Mit39	49.0	-	B>>F	
D11Mit54	56.0	F>C	B>F	♦
D11Mit60	40.0	-	B>F	♦
D11Mit61	70.0	C>>F	-	♦
D11Mit67	58.0	F>>C	-	
D11Mit70	54.0	F>>C	-	
D11Mit71	1.0	-		
D11Mit97	47.0	-	-	
D11Mit217	19.0	C>>F	B>>F	
D11Mit227		F>C		
D11Mit231	17.0	C>F	-	♦
D11Nds9	28.0	-	-	
12				
D12Mit1	3.0	-	F>>B	
D12Mit2	19.0	F>>C	F>>B	
D12Mit4	34.0	-	F>B	♦
D12Mit5	38.0	F>>C		♦
D12Mit10	6.0	-	F>B	♦
D12Mit11		F>C		
D12Mit12	10.0	C>>F	F>>B	♦
D12Mit14	38.0	-	F>>B	♦
D12Mit30	46.0	-	F>B	♦
D12Mit34	29.0	-	F>>B	♦
D12Mit36	28.0	C>F	-	♦
D12Mit76	43.0	-	-	
D12Mit88	25.0	C>>F	-	♦
D12Mit101	50.0	F>>C	-	♦
D12Mit114	29.0	-	B>>F	
D12Mit118	45.0	-	B>>F	
D12Mit121	46.0	-	F>B	
D12Mit149	38.0	C>>F	B>>F	
D12Mit159	37.0	-	-	
D12Mit172	22.0	C>F		
D12Mit178	43.0	-	-	
D12Mit182	3.0	-		
D12Mit194	45.0	F>>C		
D12Nds2	60.0	F>>C		

13				
D13Mit3	9.0	C>F	F>>B	♦
D13Mit11	38.0	-	F>B	♦
D13Mit13	33.0	F>C	-	♦
D13Mit16	0.5	C>>F		
D13Mit17	9.0	-	B>>F	♦
D13Mit19	23.5	-	F>B	♦
D13Mit23	33.0	F>C	-	♦
D13Mit35	72.0	F>>C	-	♦
D13Mit76	59.0	-	B>F	♦
D13Mit130	59.0	C>>F		♦
D13Mit221	29.0	C>>F		♦
14				
D14Mit18	16.5	C>F	F>B	♦
D14Mit39	30.0	F>>C	-	
D14Mit41		C>>F	-	
D14Mit42	52.0	-	-	
D14Mit44	10.0	C>F		♦
D14Mit75	54.0	-		
D14Mit84	21.5	-	-	
D14Mit95	54.0	F>>C	F>>B	
D14Mit97	58.0	C>F	B>F	♦
D14Mit165	52.0	F>C		
D14Mit203	28.5	-	F>B	♦

Table 2 (continued)

15	Cm	C	B	Pg
D15Mit1	47.5	-	F>B	
D15Mit2	40.4	-	B>>F	
D15Mit3	39.0	-	B>F	♦
D15Mit8	18.9	C>F	-	♦
D15Mit12	6.4	-	-	
D15Mit13	6.7	-	-	
D15Mit14	56.8	F>C	-	
D15Mit15	57.1	C>F	F>B	♦
D15Mit16	58.9	F>>C	F>>B	
D15Mit17	32.0	F>C	-	
D15Mit18	15.6	C>F	-	
D15Mit34	51.6	-	-	
D15Mit35	57.6	C>>F	B>F	♦
D15Mit39	58.3	-	-	
D15Mit42	55.5	F>>C	-	
D15Mit44	55.4	F>C	F>B	♦
D15Mit52	13.0	C>>F	B>F	♦
D15Mit53	12.3	-	F>>B	
D15Mit63	33.5	F>C		
D15Mit67	35.3	-	B>F	♦
D15Mit72	45.9	-	-	
D15Mit74	55.6	-	-	
D15Mit76	53.2	-	F>B	♦
D15Mit77	55.6	-	-	
D15Mit79	65.5	-	-	
D15Mit92	35.3	-	B>F	
D15Mit108	52.5	-	B>>F	
D15Mit111	17.8	C>>F	-	
D15Mit130	14.5	-	-	
D15Mit147	52.4	-	B>>F	♦
D15Mit154	22.2	-	B>>F	♦
D15Mit172	57.8	-	B>>F	
D15Mit173	63.4	-	-	
D15Mit175	10.1	F>>C		
D15Mit191	51.7	-	-	
D15Mit192	52.3	-	B>>F	
D15Mit193	60.0	F>C	-	♦
D15Mit217	57.8	-	F>>C	
D15Mit244	58.9	-	F>B	

16	Cm	C	B	Pg
D16Mit3	21.0	-	-	
D16Mit4	26.0	F>>C	F>>B	
D16Mit5	38.0	C>F	-	♦
D16Mit6	57.0	-	-	
D16Mit12	26.2	F>>C		
D16Mit15	30.0	F>>C	-	
D16Mit19	54.0	F>>C	F>>B	
D16Mit31	10.7	-	-	
D16Mit38	28.0	-	B>F	♦
D16Mit47	44.3	C>F	-	
D16Mit48	42.0	C>F	-	♦
D16Mit50	52.0	C>>F	B>>F	
D16Mit64	38.0	C>>F	B>>F	
D16Mit70	57.0	-	B>>F	
D16Mit71	72.0	F>C	F>B	♦
D16Mit88	9.7	C>F	-	♦
D16Mit131	6.8	C>F	F>B	♦
D16Mit132		F>C	F>B	♦
D16Mit136		C>F		♦
D16Mit154	3.4	C>F		♦
D16Nds2	28.0	-	-	
17				
D17Mit9	29.4	C>F	B>F	♦
D17Mit18	4.0	-	-	
D17Mit19		-	-	♦
D17Mit31		F>>C		
D17Mit41	53.0	-	-	
D17Mit42	47.4	-	-	
D17Mit45	16.4	C>>F	B>>F	♦
D17Mit93	44.5	-		
D17Mit102	9.8	-	B>>F	
D17Mit106	24.5	C>F	B>F	♦
D17Mit133	10.4	-	B>>F	
D17Mit135	17.0		F>B	♦
D17Mit155	55.7	C>>F		
D17Mit164		-		♦
D17Mit180	29.4	F>C		♦
D17Mit221	56.7	C>>F	B>F	♦

Table 2 (continued)

18				
D18Mit3	54.0	-	-	
D18Mit4	57.0	-	B>F	♦
D18Mit14	18.0	C>F	-	♦
D18Mit19	2.0	C>>F	-	♦
D18Mit21	6.0	C>>F		
D18Mit27	13.0	-	-	
D18Mit31	4.0	F>C	F>B	♦
D18Mit33	44.0	F>>C	-	
D18Mit34	12.0	C>>F		♦
D18Mit60	16.0	F>>C	-	
D18Mit65	2.0	-	-	
D18Mit123	31.0	C>F	-	♦
19				
D19Mit1	52.0	-	F>>B	♦
D19Mit11	41.0	-	F>>B	♦
D19Mit13	33.0	-	F>>B	
D19Mit15	16.4	-	-	
D19Mit28	12.0	-	F>>B	
D19Mit31	7.0	-	F>B	
D19Mit40	25.0	F>>C	-	
D19Mit41	16.0	C>>F	B>>F	
D19Mit43	0.0	-	-	
D19Mit61	9.8	-	-	
D19Mit68	3.3	-	B>>F	♦
D19Mit71	55.7	F>>C		♦
D19Mit79	8.7	F>C		♦
D19Mit85		C>F	F>B	♦
D19Mit88	24.0	C>>F		♦
D19Mit91	35.0	F>>C		
X				
DXMit79	56.0	C>F		
DXMit121	66.0	-	B>F	♦
DXMit124	3.0	C>F		♦
DXMit140	19.0	C>F		

Source: Neuhaus IM, Sommardahl CS, Johnson DK, Beier DR: Microsatellite DNA variants between the FVB/N and C3HeB/FeJLe and C57BL/6J mouse strains. Mammalian Genome 8:506-509, 1997.

Modifier Gene Detection and Interval Mapping in the *orpk* Mouse

Experimental design and phenotype scoring

Mice hemizygous for *TgN737Rpw* (*Tg737/+*) were selected from within the *orpk*-F line and mated to C3H mice to obtain F1 progeny. These progeny were genotyped at 21-24 days of age for *TgN737Rpw* and the mice that carried the transgene were saved for the backcross and intercross matings. The backcross was established between *Tg737/+ orpk*-F and F1 animals, the intercross was established between *Tg737/+* F1 animals. All progeny from these matings were genotyped at 21-24 days of age for *Tg737.* For the initial genome scan, 100 backcross progeny and 200 F2 progeny that were homozygous for the transgene (*Tg737/Tg737*) were scored for the selected quantitative traits. These mice were sacrificed at 27-35 days of age for the phenotype scoring. To assess the severity of the kidney and liver phenotypes, the percentage of the kidney that is cystic was measured as the kidney score and serum concentration of ALP was measured as the liver score. Blood was collected postmortem via a cardiac puncture, and serum ALP concentration was measured by automated biochemical analysis to obtain the liver score. A section of liver and kidney was placed in 10% formalin for histological examination. The remainder of the liver and the spleen were collected and snap frozen for DNA isolation. Hematoxylin and eosin stained histological sections of kidney were used for morphometric analysis of the kidney lesion. The percentage of the total area of kidney that is cystic was measured using a computerized imaging system connected to a videoscope (Bioquant, Nashville, TN). A cross-section and a longitudinal section

of kidney were measured from each animal and the cystic percentages of these two sections were summed to obtain the total percentage of cystic kidney (kidney score). The distribution of the kidney and liver scores for the backcross progeny analyzed have a mean that falls between the scores for the parental strains as expected (Fig. 14). When comparing the kidney and liver scores for individual animals, we found that there is not a correlation between the kidney score and the liver score indicating that these traits may have different modifying genes.

PCR-based genotyping

Selective genotyping of the backcross progeny was used to expedite the detection of the chromosomal location of the modifier genes that vary the severity of the kidney and liver phenotypes. An end-mapping strategy was initially utilized to determine which chromosomes might contain a QTL. This strategy generates a series of chromosomal haplotypes for each selected progeny by typing only markers at the ends of each chromosome and provides an efficient method for excluding chromosomes that are unlikely to carry a QTL [74;90]. This method is based on the fact that in affected animals carrying recessive mutations or QTL; the chromosomal interval in which the QTL resides must be homozygous for the affected (recessive) parental allele somewhere along its length. This interval will be heterozygous along its length if an affected mouse carries a nonrecombinant chromosomal interval from the unaffected (dominant) parental strain and that chromosome cannot carry the QTL. The twenty backcross progeny with the highest scores for the kidney and liver traits were typed using this method to generate a cohort of candidate chromosomes for more detailed analysis.

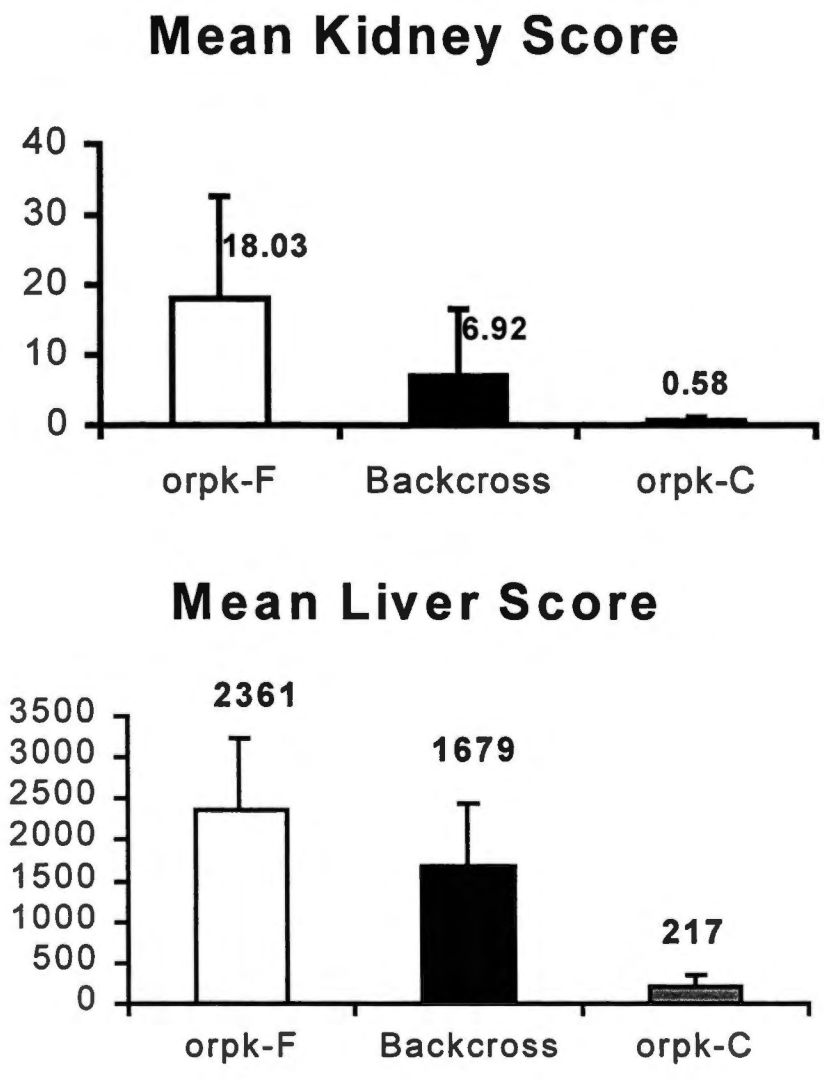

Figure 14. Mean kidney scores (top) and liver scores (bottom) for the backcross progeny and the parental strains. Mean values are presented at the top of each column and bars indicate the standard deviation of the mean.

Selective genotyping was then performed with markers spaced 10-15 cM along these chromosomes with the twenty progeny with the highest scores and the twenty progeny with the lowest scores to confirm the presence of modifier loci.

Microsatellite markers whose FVB/N and C3H alleles differed in size by at least 6 base pairs (bp) and that mapped to within 10 cM of the distal and proximal ends of each chromosome were chosen for the end-mapping strategy. Markers that mapped to 10-15 cM intervals spaced along the candidate chromosomes were chosen for the low resolution interval mapping study. These microsatellite markers were chosen from the list of microsatellite markers that were determined to be variant between the two strains. PCR primer pairs for these markers were purchased from Research Genetics, Inc. (Huntsville, AL, USA). Genomic DNA was prepared from tail clips or liver tissue according to standard protocols. PCR amplification was performed as described in the previous section for each marker.

Analysis of genetic data and QTL analysis

Genotyping data obtained by analyzing the 20 backcross progeny with the highest kidney scores and the 20 backcross progeny with the highest liver scores for the markers known to map to the ends of each autosome were analyzed with a software program developed by Neuhaus and Beier for interval haplotype analysis [90]. The nonrandom distribution of haplotypes was evaluated by X^2 analysis. The randomness of loci distribution is normalized within a data set by calculating it as a fraction of the maximum possible X^2 (%max X^2) [90]. The chromosomal intervals with a %max X^2 value of > 0.60 were identified as candidates for further analysis. This threshold was chosen based on the results

described for this type of analysis with the average %max X^2 value for intervals carrying the selected homozygous loci was O.98, while the average %max X^2 for the chromosomal intervals carrying unlinked loci was 0.40 [90]. For further analysis of the candidate chromosomes, the 20 lowest scored progeny were genotyped for the end markers and all 40 animals in each trait set were genotyped for an additional 2-3 markers within each interval depending on the size of the interval. This genotyping data and quantitative trait scores were analyzed initially using Map Manager QTb1968k [91]. To perform a more accurate analysis, the data were analyzed using the latest version of Mapmaker/QTL 1.1b [66]. These programs determine a maximum likelihood linkage map and then use an interval mapping method to define the most likely position and effects of a hypothesized QTL.

Results

Interval haplotype analysis of the genotyping data from the end mapping strategy for the 20 backcross progeny with the most severe cystic kidneys (kidney scores ranging from 11.9% to 66.2%) identified seven chromosomal intervals that may carry a candidate QTL. The 20 backcross progeny with the mildest cystic kidneys (kidney scores ranging from 0.07% to 0.7%) were then genotyped for the end markers and all 40 extreme progeny were genotyped for two to three additional markers within the interval. Linkage analysis to individual chromosomes was performed with Map Manager QTb and there were two chromosomes found to have markers linked to the most severe cystic kidney phenotype found in the backcross progeny. Three markers at the distal end of

chromosome 4 have a significance of association (P<0.05); D4Mit16, D4Mit 54, and D4Mit234. These markers flank an interval of 14 cM. Two markers at the distal end of chromosome 17 have a significance of association (P<0.05) on linkage analysis; D17Mit185 and D17Mit155. These two markers flank an interval of 14 cM. The backcross progeny genotype data and kidney scores were then analyzed using the Mapmaker/QTL program for the low-resolution interval mapping [66]. A LOD score threshold of 1 was used to identify intervals that segregate with the quantitative trait. Inheritance of a FVB/N locus on chromosome 4 correlates with increased kidney score, with a X^2 of 12.158 and a lod score of 2.64 for the interval between D4Mit54 and D4Mit234 (Fig. 15). This 5 cM interval explains 16.4% of the variance for kidney score in affected backcross progeny. Inheritance of a FVB/N locus on chromosome 13 also correlates with increased kidney score, with a X^2 of 6.705 and a lod score of 1.46 for the interval between D13Mit130 and D13Mit77 (Fig. 16). This 12 cM interval explains 12.1% of the variance for kidney score in affected backcross progeny. Inheritance of a FVB/N locus on chromosome 17 correlates with increased kidney score, with X^2 of 7.641 and a lod score of 1.66 for the interval D17Mit185 and D17Mit155 (Fig. 17). This 15 cM interval explains 13.9% of the variance for kidney score in affected backcross progeny. Selective genotyping was performed with the 40 extreme F2 progeny for the markers on chromosomes 4,13, and 17. Linkage analysis using Map Manager QTb with this data showed the same three markers on distal chromosome 4 to have a significance of association (P<0.05) with the severe cystic kidney phenotype.

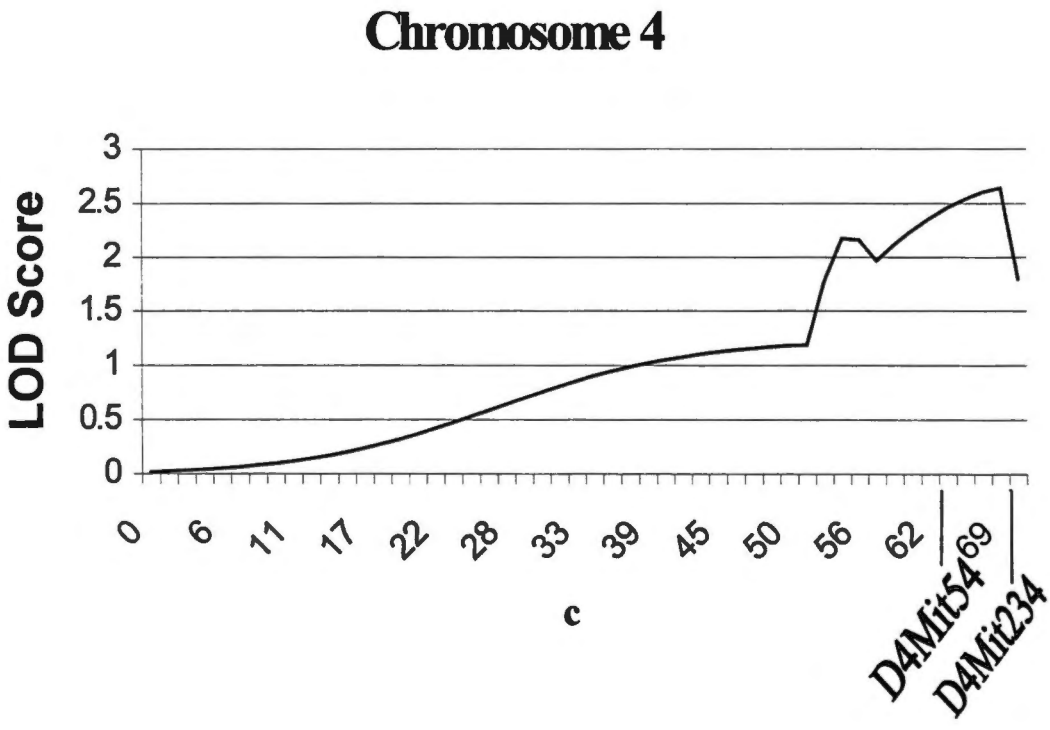

Figure 15. LOD score values for intervals on chromosome 4 associated with cystic kidney disease severity in affected *orpk* mice, calculated according to Mapmaker/QTL.

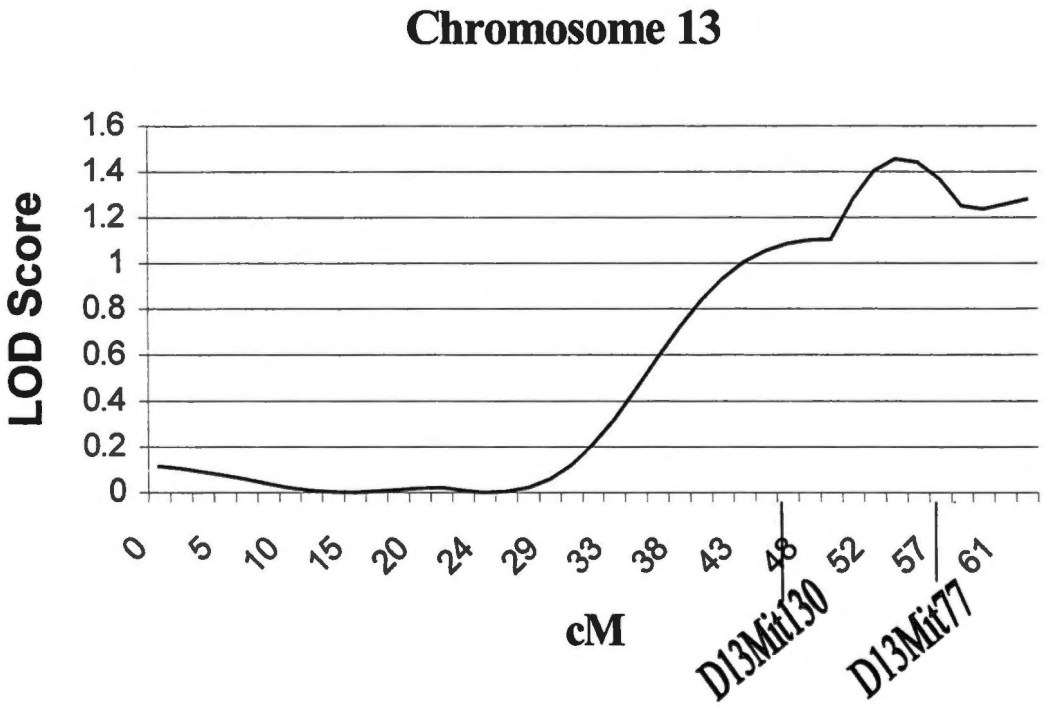

Figure 16. LOD score values for intervals on chromosome 13 associated with cystic kidney disease severity in affected *orpk* mice, calculated according to Mapmaker/QTL.

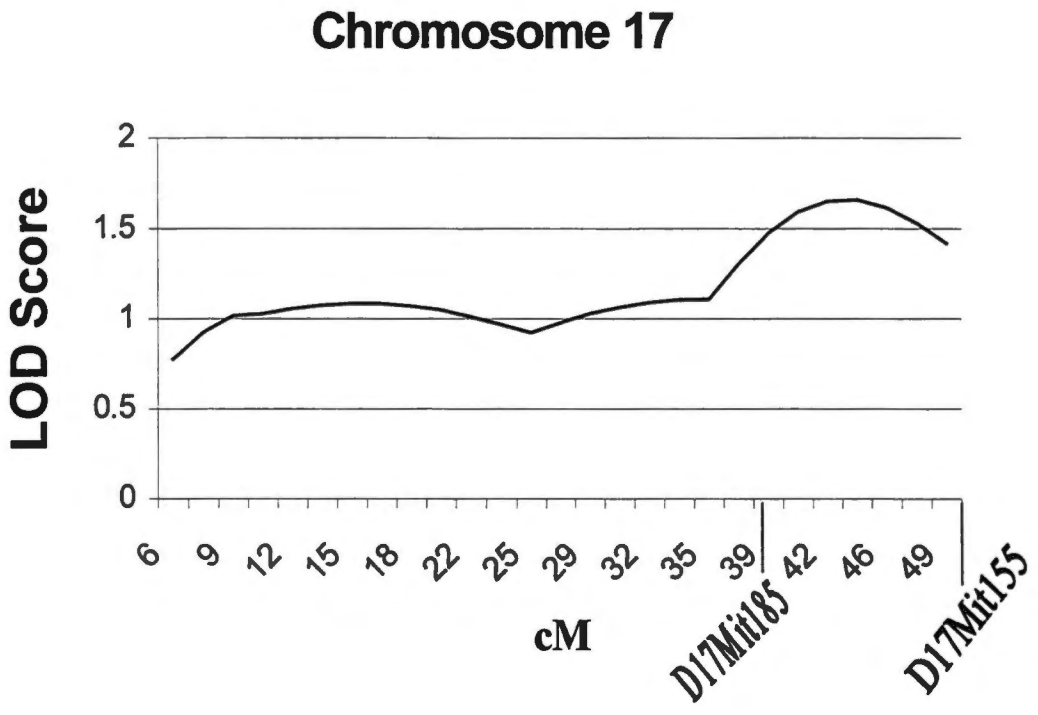

Figure 17. LOD score values for intervals on chromosome 17 associated with cystic kidney disease severity in affected *orpk* mice, calculated according to Mapmaker/QTL.

Interval haplotype analysis of the genotyping data from the end mapping strategy for the 20 backcross progeny with the highest serum ALP concentrations (liver score ranging from 2452 to 3920) identified 5 chromosomal intervals that may carry a candidate QTL. The 20 backcross progeny with the lowest serum ALP concentrations (liver scores ranging from 279 to 791) were then genotyped for the end markers, and all 40 extreme progeny were genotyped for two to three additional markers within the interval. The data was analyzed with Map Manager QTb for linkage to individual chromosomes. The proximal marker on chromosome 9, D9Mit43, was found to have a significance of association ($P<0.05$) with the backcross progeny having the highest serum ALP concentrations. Low-resolution interval mapping was performed using the liver scores and genotyping data with Mapmaker/QTL program. A LOD score threshold of 1 was set to identify intervals that segregate with the quantitative trait. No significant intervals were found on this initial analysis.

Discussion

In stage 1 of our QTL analysis to detect potential modifier loci of the cystic kidney phenotype, analysis of separate populations of severely affected and mildly affected mice in the backcross progeny identified possible modifying loci on chromosomes 4, 13 and 17. A significant association of a recessively inherited FVB/N-related locus on all three chromosomes with cystic kidney disease severity was found. This confirms our hypothesis that there are several modifying loci that influence the kidney phenotype between the C3H and FVB/N

strains. Stage 2, the low-resolution interval mapping stage, was performed using the Mapmaker/QTL program, because it is better designed to analyze the extreme population data obtained by selective genotyping. It is possible that inheritance of each of these loci contributes to the variance in disease severity seen. Inheritance of one or more of these loci may result in the more severe cystic kidney phenotype as a result of a direct or indirect interaction between their protein products and the *Tg737* protein product. The interval that explains most of the variance is at the distal end of chromosome 4 and has been found to span an interval of 3 cM between D4Mit 54 and D4Mit 234. The lod score for association with increased cystic kidney score for the backcross progeny was found to be 2.64, which is consistent with linkage. This interval was also identified when analyzing the genotyping and the kidney score data from the F2 extreme progeny using the Map Manager QTb program for linkage analysis. The fact that the markers for this interval segregated with the severe kidney scores with both populations makes it a strong candidate to contain a modifier gene. A modifier locus that strongly modulates the progression of the polycystic kidney phenotype in *pcy* and *cpk* mice was also mapped to chromosome 4 [83;84]. However, this locus is 30 cM proximal to the locus identified in our search. Further analysis of all three intervals will be performed by genotyping more backcross and F2 progeny for the flanking markers to strengthen the LOD score of association for each interval. Also, markers identified as polymorphic between the parental strains and that map within the intervals will be used to further define the interval.

The search for modifier loci that control the liver trait detected a nonrandom segregation of one marker on chromosome 9 that segregated with the highest

liver scores. Low-resolution interval mapping using the Mapmaker/QTL program failed to identify any significant associations, however. This is felt to be due to the small number of animals being used in the analysis, and possible to weaker modifier loci. Further analysis using more backcross progeny will be performed for the chromosomal intervals identified by interval haplotype analysis. Increasing the number of animals genotyped for the selected markers flanking these chromosomal intervals should strengthen the ability to identify modifier loci. We hypothesize that the modifier loci will be different for the liver and kidney traits since there is not a correlation between the kidney score and the liver score for the backcross progeny or F2 progeny analyzed.

V. SUMMARY

The aim of determining the effect of paclitaxel on cystic kidney and liver lesions in the *orpk* mutant line lead to several conclusions. Taxol has no effect on the cystic kidney disease progression in the *orpk* mutants at a dose effective in the *cpk* mutants. Taxol has no effect on the targeting of the EGFR in the renal cystic epithelial cells. Taxol has no effect on the proliferation and dedifferentiation of the biliary ductules in the *orpk* mutants. These results may be due to the differences in the two mutations at the molecular and cellular levels. Also, the disease conditions have a different progression of the renal pathology, and different multiorgan histopathology. In addition, the *orpk* mutation is on the FVB/N genetic background while the *cpk* mutation is on a C57BL/6 genetic background, raising the possibility that genetic background may have an influence on the effectiveness of taxol as a therapeutic agent. Additional experiments with the *orpk* mutation on the C57BL/6 would address this possibility. Since publication of our study in Pediatric Nephrology 11:728-733, 1997; taxol has been shown to have no effect on the progression of PKD in the Han:SPRD-Cy rat model of PKD nor in the *pcy* mouse model of PKD [56]. On the basis of these three studies in rodents, it appears that taxol has limited potential usefulness as a therapeutic agent in the treatment of PKD.

The aim of identifying the phenotypic variations of the *orpk* mutation on the C3H genetic background showed major phenotypic variations in the kidney, liver, and pancreatic lesions. The significant differences in the lesions suggest the presence of important modifier genes that vary in the FVB/N and C3H genetic

backgrounds. These differences were evident in the first generation backcross to C3H indicating that the modifier genes may be dominant in the C3H background. Percent of the kidney area that is cystic was selected as a quantitative trait reflecting the kidney phenotype and serum concentration of ALP was selected as a quantitative trait reflecting the liver phenotype since there was significant differences in these values between the *orpk*-F and *orpk*-C mutant animals. These quantitative traits were utilized to identify the chromosomal location of the modifier genes.

The aim of identifying the chromosomal location of the modifier genes that vary the cystic kidney phenotype between the C3H and FVB/N genetic backgrounds has been accomplished. The next step is to begin Stage 3 of the QTL analysis, the single-QTL-oriented fine mapping stage. The basis for this stage is analysis of recombinants within an interval previously found to contain the modifier gene. The experimental designs for this stage require the generation of thousands of progeny; therefore, is a very lengthy process. Since the ultimate goal is to get from fine mapping to the gene itself, therefore an alternative to linkage analysis, is to search for expressed sequences mapping within the intervals found to contain modifier loci. This approach requires the region to be defined to < 1 cM and can still be difficult if many genes map to the region. Potential candidates identified can be tested for expression patterns appropriate for the kidney phenotype. In addition, DNA sequencing will identify polymorphisms between the C3H and FVB/N alleles of any candidate gene. An initial search of databases available for the mouse genome has been performed for the chromosomal intervals identified to contain potential modifier loci of the cystic kidney phenotype. There are several genes within each interval that could

be a candidate modifier, but not one that is an obvious standout. Within the strongest interval on chromosome 4, between D4Mit54 and D4Mit234, there are cell division cycle genes, G-protein related genes, and phospholipase A2 genes that could play a role in the pathogenesis of the cyst formation via cell signaling pathways. This region shows conserved synteny with the human chromosomal region 1p36-34, and this human chromosomal region also contains many genes that could play a role in cystogenesis. Further narrowing of the interval and research on the genes within the interval are needed before a candidate gene can be identified. The aim for the future of this project is to identify these candidate genes and prove their function as modifiers of the *orpk* cystic kidney phenotype. Identification of modifier genes will provide information into the pathogenesis of polycystic kidney disease. Understanding of the molecular and cellular nature of these modifying genes can lead to targets for diagnostics or therapeutics for polycystic kidney disease.

Reference List

Reference List

1. Peterson JC: Gross anatomical studies of a newborn infant with the Meckel syndrome. Am.J.Med.Genet. 18:649-659, 1984

2. Fick GM, Gabow PA: Heredity and acquired cystic disease of the kidney. Kidney Int. 46:951-964, 1994

3. Grantham JJ: Polycystic kidney disease: heredity and acquired. Ann.Rev.Med. 38:409-420, 1993

4. Gabow PA: Autosomal dominant polycystic kidney disease. N.Eng.J.Med. 329:332-342, 1993

5. Dalgaard OZ: Bilateral polycystic disease of the kidneys: a follow-up of two hundred and eighty-four patients and their families. Acta.Med.Scand.Suppl. 328:1-255, 1957

6. Gabow PA: Autosomal dominant polycystic kidney disease. Am.J.Kidney Dis. 22:511-512, 1993

7. Simon EA, Cook S, Davisson MT, D'Eustchio P, Guay-Woodford LM: The mouse congenital polycystic kidney (*cpk*) locus maps within 1.3 cM of the chromosome 12 marker D12Nyu2. Genomics 21:415-418, 1994

8. Bernstein J, Gardner KD: Renal cystic disease and renal dysplasia, in Campbell's Urology, edited by P.C.Walsh etal, Philadelphia, W. B. Saunders, 1986, pp 1760-1818

9. Lippert MC: Renal Cystic Disease, in Adult and Pediatric Urology, edited by Gillenwater JY, Chicago, Mosby, 1991, pp 711-743

10. Zerres KG, Mucher G, Bachner L, et.al: Mapping of the gene for autosomal recesive polycystic kidney disease (ARPKD) to chromosome 6p21-cen. Nat.Genet. 7:429-432, 1994

11. Zerres KG, Rudnik-Schoneborn S: On genetic heterogeneity, anticipation and imprinting in polycystic kidney diseases {editorial}. Nephrol.Dial.Transplant 10:7-9, 1995

12. Gattone VH, Grantham JJ: Understanding human cystic disease through experimental models. Semin.Nephrol. 11:617-631, 1991

13. Gattone VH, Kraybill AL, Gudapaty S, et.al: Autosomal dominant polycystic kidney disease (ADPKD) in the rat. J.Am.Soc.Nephrol. 1:629, 1990

14. Schafer K, Gretz N, Bader M: Characterization of the Han:SPRD rat model for hereditary polycystic kidney disease. Kidney International 46:134-152, 1994

15. Grantham JJ: Pathogenesis of renal cyst expansion: opportunities for therapy. Am.J.Kidney Dis. 23:210-218, 1994

16. Atala A, Freeman MR, Mandell J, Beier DR: Juvenile cystic kidneys (*jck*): a new mouse mutation which causes polycystic kidneys. Kidney International 43:1081-1085, 1993

17. Avner ED, Studnicki FE, Young MC, et.al.: Congenital murine polycystic kidney disease I. The ontogeny of tubular cyst formation. Pediatr.Nephrol.587-596, 1987

18. Avner ED, Sweeney WE, Young MC, et.al.: Congenital murine polycystic kidney disease II. Pediatr.Nephrol. 2:210-218, 1988

19. Carone FA, Bacallao R, Kanware YS: Biology of polycystic kidney disease. Lab.Invest. 70:750-753, 1994

20. Takahashi H, Calvet JP, Dittemore-Hoover D, et.al.: A hereditary model of slowly progressive polycystic kidney disease in the mouse. J.Am.Soc.Nephrol. 1:980-989, 1991

21. Flaherty L, Bryda EC, Collins D, et.al.: New mouse model for polycystic kidney disease with both recessive and dominant gene effects. Kidney Int. 47:552-558, 1995

22. Ozawa Y, Nauta J, Sweeney WE, Avner ED: A new murine model of autosomal recessive polycystic kidney disease. Nippon Jinzo Gakikai Shi 35:349-354, 1993

23. Nagao S, Hibino T, Koyama Y, et.al: Strain difference in expression of the adult-type polycystic kidney gene, pcy, in the mouse. Jikken Dobutsu 40:45-53, 1991

24. Calvet JP: Injury and development in polycystic kidney disease. Curr.Opin.Nephrol.Hypertens. 3:340-348, 1994

25. Nauta J, Ozawa Y, Sweeney WE, Avner ED, et.al: Renal and biliary abnormalities in a new murine model of autosomal recessive polycystic kidney disease. Pediatr.Nephrol. 7:163-172, 1993

26. Moyer JH, Lee-Tischler MJ, Kwon HY, Schrick JJ, Avner ED, Sweeney WE, Godfrey VL, Cacheiro NLA, Wilkinson JE, Young MC: Candidate gene associated with a mutation causing recessive polycystic kidney disease in mice. Science 264:1329-1333, 1994

27. Yoder BK, Richards WG, Sommardahl CS, Sweeney WE, Michaud EJ, Wilkinson JE, Avner ED, Woychik RP: Functional correction of renal defects in a mouse model for ARPKD through expression of the cloned wild-type *Tg737* cDNA. Kidney Int. 50:1240-1248, 1996

28. Richards WG, Yoder BK, Isfort RJ, Detilleux PG, Foster C, Neilsen N, Woychik RP, Wilkinson JE: Oval cell proliferation associated with the murine insertional mutation *TgN737Rpw*. Am. J. Path. 149:1919-1930, 1996

29. Yoder BK, Richards WG, Sommardahl CS, Sweeney WE, Michaud EJ, Wilkinson JE, Avner ED, Woychik RP: Differential rescue of the renal and hepatic disease in an autosomal recessive polycystic kidney disease mouse mutant: *A new model to study the liver lesion*. Am. J. Path. 150:2231-2241, 1997

30. The International Polycystic Kidney Disease Consortium.: Polycystic kidney disease: the complete structure of the PKD1 gene and its protein. Cell 81:289-298, 1994

31. Mochizuki T, Wu G, Hayashi T, Xenophontos SL, Veldhuisen B, Saris JJ, Reynolds DM, Cai Y, Gabow PA, Pierides A, Kimberling WJ, Breuning M, Deltas CC, Peters DJ, Somlo S: PKD2, a gene for polycystic kidney disease that encodes an integral membrne protein. Science 272:1339-1342, 1996

32. Mucher G, Becker J, Knapp M, Buttner R, Moser M, Rudnik-Schoneborn S, Somlo S, Germino GG, Onuchic LF, Avner ED, Guay-Woodford LM: Fine mapping of the autosomal recessive polycystic kidney disease locus (*PKHD1*) and the genes MUT, RDS, CSNK2 beta, and GSTA1 at 6p21.1-p12. Genomics 48:40-45, 1998

33. Lamb JR, Michaud WA, Sikorski RA, Hieter PA: Cdc16p, Cdc23p and Cdc27p form a complex essential for mitosis. EMBO J 13:4321-4328, 1994

34. Becker W, Kentrup H, Klumpp S, Schultz JE, Joost HG: Molecular cloning of a protein serine/threonine phosphatase containing a putative regulatory tetratricopeptide repeat domain. J.Biol.Chem. 269:22586-22592, 1994

35. Mirabito PM, Morris NR: BIMA, a TPR-containing protein required for mitosis, localizes to the spindle pole body in *Aspergillus nidulans*. J.Cell Biol. 120:959-968, 1993

36. Yoder BK, Wilkinson JE, Avner ED, Woychik RP: Tg737 protein interacts with polycystin and proteins controlling epithelial polarity, EGFR stability and cellular differentiation. J.Am.Soc.Nephrol. 8: 1997

37. Murcia NS, Sweeney WE, Avner ED: New insights into the molecular pathophysiology of polycystic kidney disease. Kidney Int. 55:1187-1197, 1999

38. Murcia NS, Woychik RP, Avner ED: The molecular biology of polycystic kidney disease. Pediatr.Nephrol. 12:721-726, 1998

39. Rowinsky EK, Donehower RC: Paclitaxel (Taxol). N.Eng.J.Med. 332:1004-1014, 1995

40. Ebirhara I, Killen PD, Laurie GW, Huang T, Yamada Y, Martin GR, Brown KS: Altered mRNA expression of basement membrane components in a murine model of polycystic kidney disease. Lab.Invest. 58:262-269, 1988

41. Rankin CA, Suzuki K, Ioth T, Ziemer DM, Grantham JJ, Calvet JP, Nagase H: Matrix metalloproteinases and TIMPS in cultured C57BL/6J-*cpk* kidney tubules. Kidney Int. 50:835-844, 1996

42. Sullivan LP, Wallace DP, Grantham JJ: Chloride and fluid secretion in polycystic kidney disease. J.Am.Soc.Nephrol. 9:903-916, 1998

43. Tanner GA, McQuillan PF, Maxwell MR, Keck JK, McAteer JA: An in vitro test of the cell stretch-proliferation hypothesis of renal cyst enlargement. J.Am.Soc.Nephrol. 6:1230-1241, 1995

44. Avner ED, Sweeney WE, Nelson WJ: Abnormal sodium pump distribution during renal tubulogenesis in congenital murine polycystic kidney disease. Proc.Natl.Acad.Sci. 89:7447-7451, 1992

45. Grantham JJ: Polycystic kidney disease: Neoplasia in disguise. Am.J.Kidney Dis. 15:110-116, 1990

46. Nauta J, Sweeney WE, Avner ED: Epithelial hyperplasia and cell polarity abnormalities in murine autosomal recessive polycystic kidney disease. J.Am.Soc.Nephrol. 1:257, 1991

47. Wilson PD: Aberrant epithelial cell growth in autosomal dominant polycystic kidney disease. Am.J.Kidney Dis. 17:634-637, 1991

48. Cowley BDJ, Grantham JJ, Chadwick LJ, Calvet JP: Elevated proto-oncogene expression in polycystic kidneys of the C57BL/6J(cpk) mouse. J.Am.Soc.Nephrol. 1:1048-1053, 1991

49. Herrera GA: C-erb B-2 amplication in cystic renal disease. Kidney Int. 40:509-513, 1991

50. Woo DDL: Apoptosis and loss of renal tissue in polycystic kidney disease. N.Eng.J.Med. 333:18-25, 1995

51. Lanoix J, D'Agati V, Szabolcs M, Trudel M: Dysregulation of cellular proliferation and apoptosis mediates human autosomal dominant polycystic kidney disease (ADPKD). Oncogene 13:1160, 1996

52. Gattone VH, Andrews.G.K., Niu FW, Chadwick LJ, Klein RM, Calvet JP: Defective epidermal growth factor gene expression in mice with polycystic kidney disease. Dev.Biol. 138:225-230, 1990

53. Orellana SA, Sweeney WE, Neff CD, Avner ED: Epidermal growth factor receptor is abnormal in murine polycystic kidney. Kidney Int. 47:490-499, 1995

54. Richards WG, Sweeney WE, Yoder BK, Wilkinson JE, Woychik RP, Avner ED: Epidermal growth factor receptor activity mediates renal cyst formation in polycystic kidney disease. J. Clin. Invest. 101:935-939, 1998

55. Woo DDL, Miao SYP, Pelayo JC, Woolf AS: Taxol inhibits progression of congenital polycystic disease. Nature 368:750-753, 1994

56. Martinez JR, Cowley BD, Gattone VH, Nagao S, Yamaguchi T, Kaneta S, Takahashi H, Grantham JJ: The effect of paclitaxel on the progression of polycystic kidney disease in rodents. Am.J.Kidney Dis. 29:435-444, 1997

57. Sommardahl CS, Woychik RP, Sweeney WE, Avner ED, Wilkinson JE: Efficacy of taxol in the *orpk* model of polycystic kidney disease. Pediatr.Nephrol. 11:728-733, 1997

58. Aukema HM, Housini I, Rawling JM: Dietary soy protein effects on inherited polycystic kidney disease are influenced by gender and protein level. J.Am.Soc.Nephrol. 10:300-308, 1999

59. Yamaguchi T, Valli VE, Philbrick D, Holub B, Yoshida K, Takahashi H: Effects of dietary supplementation with n-3 fatty acids on kidney morphology and the fatty acid composition of phospholipids and triglycerides from mice with polycystic kidney disease. Res. Commun. Chem. Pathol. Pharmacol. 69:335-351, 1990

60. Sweeney WE, Futey L, Frost P, Avner ED: In vitro modulation of cyst formation by a novel tyrosine kinase inhibitor. Kidney Int. 56:406-413, 1999

61. Lander ES, Schork NJ: Genetic dissection of complex traits. Science 265:2037-2048, 1994

62. Tanksley SD: Mapping Polygenes. Annu.Rev.Genet. 27:205-233, 1993

63. Darvasi A: Experimental strategies for the genetic dissection of complex traits in animal models. Nat.Genet. 18:19-24, 1998

64. Dietrich W, Katz H, Lincoln SE, et.al: A genetic map of the mouse suitable for typing intraspecific crosses. Genetics 131:423-447, 1992

65. Dietrich W, Miller JC, Steen RG, et.al: A genetic map of the mouse with 4,006 simple sequence length polymorphisms. Nat.Genet. 7:220-245, 1994

66. Lander ES, Botstein D: Mapping mendelian factors underlying quantitative traits using RFLP linkage maps. Genetics 121:185-199, 1989

67. Silver LM: *Mouse Genetics: Concepts and Applications*. New York, Oxford University Press, 1995, 259-305

68. Sweeney WE, Avner ED: Intact organ culture of murine metanephrons. J.Tissue Cult.Methods 13:163-168, 1991

69. Kris RM, Lax I, Gullic W, Waterfield MD, Ullrich A, Fridkin M, Schlessinger J: Antibodies against a synthetic peptide as a probe for the kinase activity of avian EGF receptor and v-erbGB protein. Cell 40:619-625, 1985

70. Blyth H, Ockenden BG: Polycystic diseases of kidneys and liver presenting in childhood. Journal of Medical Genetics 8:257-284, 1971

71. Avner ED: Renal developmental diseases. Semin.Nephrol. 13:427-435, 1993

72. Avner ED, Sweeney WE: Altered membrane localization of NaKATPase and epidermal growth factor receptor during *in vitro* modulation of collecting tubule cystogenesis. J.Am.Soc.Nephrol. 2:673, 1992

73. Harris RC: Potential physiologic roles for epidermal growth factor in the kidney. Am.J.Kidney Dis. 17:627-630, 1991

74. Iakoubova OA, Dushkin H, Beier DR: Localization of a murine recessive polycystic kidney disease mutation and modifying loci that affect disease severity. Genomics 26:107-114, 1995

75. D'Agata ID, Jones MM, Perez-Atayde AD, Guay-Woodford LM: Combined cystic disease of the liver and kidney. Semin.Liver Dis. 14:215-228, 1994

76. Kaplan BS, Fay J, Shah V, et.al: Autosomal recessive polycystic kidney disease. Pediatr.Nephrol. 3:43-49, 1989

77. Nagao S, Takahaski H: Linkage analysis of two murine polycystic kidney disease genes, *pcy* and *cpk*. Jikken Dobutsu 40:557-560, 1991

78. Fry JL, Koch WE, Jennette JC, et.al: A genetically determined murine model of infantile polycystic kidney disease. J.Urol. 134:828-833, 1985

79. Hogan BCF, Lacy E: *Manipulating the mouse embryo: A laboratory manual*. Cold Springs Harbor, Cold Springs Harbor Laboratory Press, 1986

80. Lu W, Peissel B, Babakhanlou H, Pavlova A, Fan X, Larson C, Brent G, Zhou J: Perinatal lethality with kidney and pancreas defects in mice with targetted *Pkd1* mutation. Nat.Genet. 17:179-181, 1997

81. Iakoubova OA, Dushkin H, Beier DR: Genetic analysis of a quantitative trait in a mouse model of polycystic kidney disease. Am.J.Respir.Crit.Care Med. 156:S72-S77, 1997

82. Guay-Woodford LM, Bryda EC, Christine B, Lindsey JR, Collier WR, Avner ED, D'Eustchio P, Flaherty L: Evidence that two phenotypically distinct mouse PKD mutations, *bpk* and *jcpk*, are allelic. Kidney International 50:1158-1165, 1996

83. Woo DDL, Tran T, Kurtz I: Genetic Identification of two major modifying loci that control the progression of polycystic kidney disease in the *cpk* mice. J.Am.Soc.Nephrol. 7:1609, 1996

84. Woo DDL, Nguyen DK, Khatibi N, Olsen P: Genetic identification of two major modifying loci of polycystic kidney disease in *pcy* mice. J.Clin.Invest. 100:1934-1940, 1997

85. Upadhya P, Churchill G, Birkenmeier EH, Barker JE, Frankel WN: Genetic modifiers of polycystic kidney disease in intersubspecific KAT2J mutants. Genomics 58:129-137, 1999

86. Taketo M, Schroeder AC, Morbraaten LE, Gunning KB, Hanten G, Fox RR, Roderick TH, Stewart CL, Lilly F, Hansen CT, Overbeek PA: FVB/N: an inbred strain perferable for transgenic analyses. Proc.Natl.Acad.Sci. 88:2065-2069, 1991

87. Neuhaus IM, Sommardahl CS, Johnson DK, Beier DR: Microsatellite DNA variants between the FVB/N and C3HeB/FeJLe and C57BL/6J mouse strains. Mammal. Genome 8:506-509, 1997

88. Sambrook J, Fritsch EFMT: *Molecular Cloning: A Laboratory Manual*, 2nd ed. Cold Spring Harbor, Cold Spring Harbor Laboratory Press, 1989

89. Bassam BJ, Caetno-Anolles G, Gresshoff PM: Fast and sensitive silver staining of DNA in polyacrylamide gels. Anal.Biochem. 196:80-83, 1991

90. Neuhaus IM, Beier DR: Efficient localization of mutations by haplotype analysis. Mammal. Genome 9:150-154, 1998

91. Manly KF, Elliot RW: RI manager, a microcomputer program for analysis of data from recombinant inbred strains. Mammal. Genome 1:123-126, 1991

VITA

Carla Sinor Sommardahl was born November 4, 1962 in Roanoke, Virginia to Dr. Carl H. Sommardahl, DDS and Ruthie Wasson. In 1966, her mother married Donald R. Sinor, a career Army officer. After spending her elementary years living throughout the southern United States and in Germany on army bases, her family was stationed in Columbia, SC. She became active in horseback riding and showing during the four years living in Columbia. Her parents then moved back to her mother's hometown of Harrison, AR. Carla graduated from Harrison High School and attended the University of Arkansas taking pre-veterinary courses. During her college years, she was a member of Phi Mu sorority, Mortar Board Honor Society, and graduated as the Senior Key Scholar in the College of Agriculture in 1985 with a the Bachelor of Science degree in animal science. In 1989, she graduated cum laude from Louisiana State School of Veterinary Medicine in Baton Rouge with the Doctor of Veterinary Medicine degree.

She pursued her interest in large animal medicine by completing an internship and residency at the University of Tennessee College of Veterinary Medicine in the Large Animal Clinical Sciences Department. She completed her large animal internal medicine residency program in 1994 and became board certified in large animal internal medicine in 1995. During her residency program, she began taking courses toward a Doctoral degree in the Comparative Experimental Medicine program at the University of Tennessee. She received a Center of Excellence Research Fellowship in 1994, for her work under the direction of Dr. Erby Wilkinson. She also received five year NIH Clinical Scientist Award in 1997

for her graduate work and to continue as a postdoctoral fellow after receiving her Doctorate of Philosophy degree in Comparative Experimental Medicine in December 1999.

Her professional activities include membership in the American Veterinary Medical Association, the American Association of Small Ruminant Practitioners, and Diplomat in the American College of Veterinary Internal Medicine.